A SEMI-AUTONOMOUS ROBOTIC SYSTEM FOR NEEDLE TRACKING AND VISUAL SERVOING USING 2D MEDICAL ULTRASOUND

Kim Mathiassen

December 19, 2016

Department of Informatics
Faculty of Mathematics and Natural Science
University of Oslo
Oslo, Norway

The Intervention Centre
Oslo University Hospital, Rikshospitalet
Faculty of Medicine
University of Oslo
Oslo, Norway

A thesis submitted for the degree of Doctor of Philosophy

Series of dissertations submitted to the
Faculty of Mathematics and Natural Sciences, University of Oslo
No. 1902

ISSN 1501-7710

Cover: Hanne Baadsgaard Utigard.
Print production: Reprosentralen, University of Oslo.

Abstract

The main aim of the thesis is to contribute to a semi-autonomous active sensing system for needle tracking during percutaneous needle insertion. The objective is twofold: first to develop a system for acquiring ultrasound images, then to analyze these images in order to track the needle. The thesis is thus divided into two main lines of research: (1) investigate whether it is feasible to make a robotic system for acquiring ultrasound images using commercially available components; (2) investigate how to track a needle using 2D ultrasound images and possibly other sensor information in real-time.

In this thesis we have developed an ultrasound robotic system using the UR5 robot from Universal Robots, based on a set of requirements derived from the state of the art in the literature. The system has both force and haptic control. We developed and tested several novel methods for tracking a needle in an ultrasound image. In addition, a novel visual servoing method has been developed to ensure that the needle lies in the imaging plane of the ultrasound probe during insertions.

The thesis concludes that it is feasible to make an ultrasound robotic system using commercially available components and shows that such a system meets the derived requirements. It also concludes that the novel needle tracking methods presented are both accurate and precise compared to previous methods presented in the literature. It is also shown that using velocity measurements from a needle insertion robot significantly improves the both the accuracy and precision, compared to only using ultrasound images. The visual servoing method shows promise for solving the alignment problem of keeping the needle in the imaging plane of the ultrasound probe.

Preface

This thesis is submitted to the University of Oslo for the degree of Doctor of Philosophy. The research was conducted at the Intervention Centre, Oslo University Hospital (OUS) and the Department of Informatics, University of Oslo (UiO). The main supervisor was Associate Professor Ole Jakob Elle (OUS/UiO). The co-supervisors were Associate Professor Kyrre Glette (UiO), Associate Professor Mats Høvin (UiO) and Professor Per Kristian Hol (OUS). This research was funded by the Norwegian Ministry of Education and Research and the European Union Seventh Framework Programme (FP7/2007-2013) under grant agreement no 270396 (I–SUR).

Acknowledgements

I would like to express my sincere gratitude to all my advisors for continuous support throughout my Ph.D study: Ole Jakob Elle for guiding me from the start to finish; Mats Høvin for his help with 3D printing and mechanical design; Kyrre Glette for the extra effort reviewing papers; and Per Kristin Hol for the clinical feedback and his medical expertise. My sincere thanks to all of them for their help discussing, reviewing and contributing to our results.

I am grateful for the opportunity to stay six month at the ALTAIR Robotics Lab at the University of Verona, and I am especially grateful to Paolo Fiorini for making this possible. The stay resulted in two papers with the help of Diego Dall'Alba, Riccardo Muradore and Paolo Fiorini, and I am thankful for the good collaboration and assistance with the papers.

During my PhD I was part of the Intelligent Surgical Robotics project, a project under the European Union Seventh Framework Programme. I would like to thank Ole Jakob Elle for the opportunity of being part of the project, and all the participants for sharing their knowledge and for their collaboration in the project.

I thank everyone at both the Intervention Centre at Rikshospitalet and the Robotics and Intelligent Systems group at the University of Oslo for a good working environment and their assistance with my PhD work. I particularly thank my colleagues who shared the open office with me for good discussions, enjoyable lunches and fun free time activities together. I would also thank Knut Brabrand and Trygve Syversveen from the Radiology department of Rikshospitalet for their help with understanding ultrasound imaging from a clinical perspective.

Finally, I would like to thank my wife for supporting me throughout the PhD period and never doubting for a second that I would finish.

List of Thesis Papers

Paper I **An Ultrasound Robotic System Using the Commercial Robot UR5**
Kim Mathiassena, Jørgen Enger Fjellin, Kyrre Glette, Per Kristian Hol and Ole Jakob Elle
Frontiers in Robotics and AI, vol 3, 2016

Paper II **Real-Time Biopsy Needle Tip Estimation in 2D Ultrasound Images**
Kim Mathiassen, Diego Dall'Alba, Riccardo Muradore, Paolo Fiorini and Ole Jakob Elle
Robotics and Automation (ICRA), 2013 IEEE International Conference on, pages 4363–4369, May 2013.

Paper III **Robust Real-Time Needle Tracking in 2D Ultrasound Images using Statistical Filtering**
Kim Mathiassen, Diego Dall'Alba, Riccardo Muradore, Paolo Fiorini and Ole Jakob Elle
IEEE Transactions on Control System Technology, Accepted

Paper IV **Visual Servoing of a Medical Ultrasound Probe for Needle Insertion**
Kim Mathiassen, Kyrre Glette, and Ole Jakob Elle
Robotics and Automation (ICRA), 2016 IEEE International Conference on, pages 3426-3433, May 2016.

Contents

Abstract **iii**

Preface **v**

Acknowledgements **vii**

List of Thesis Papers **ix**

Contents **xi**

1 Introduction **1**
- 1.1 Aims 2
- 1.2 Outline 2

2 Background **5**
- 2.1 Ultrasound-guided interventions 5
- 2.2 Robotic ultrasound systems 10
- 2.3 Needle tracking in US images 17
- 2.4 Visual servoing of US probe 19
- 2.5 Needle placement robots 23

3 Materials, Methods and Software **25**
- 3.1 Materials 25
- 3.2 Methods 26
- 3.3 Software 28

4 Research contribution **29**
- 4.1 Paper I 31
- 4.2 Paper II 32
- 4.3 Paper III 34
- 4.4 Paper IV 36

5 Discussion **39**
- 5.1 Approaches and design choices 39
- 5.2 Performance 40
- 5.3 Limitations 42
- 5.4 Impact 43

6 Conclusion **45**
6.1 Future work 45

Bibliography **47**

Papers **57**
I An Ultrasound Robotic System Using the Commercial Robot UR5 57
II Real-Time Biopsy Needle Tip Estimation in 2D Ultrasound Images 75
III Robust Real-Time Needle Tracking in 2D Ultrasound Images using Statistical Filtering 85
IV Visual Servoing of a Medical Ultrasound Probe for Needle Insertion 101

Chapter 1

Introduction

The use of robots in health care has dramatically increased over the last decade. A great deal of research has been conducted using robots in different areas of health care, from surgical robots [26] to robots used for patient rehabilitation [42]. This thesis is related to autonomous percutaneous needle insertion by using robots. This is a complex task and this thesis addresses only a part of that challenge, namely how to track the needle while it is inside the patient. First we provide a short explanation of the medical context of a needle insertions, and how to automate the task, before presenting the exact research topics of the thesis.

Medical ultrasound is an important imaging modality in modern medicine and is widely used in both diagnostics and treatment. Percutaneous needle insertion, meaning inserting a needle through the skin, is a very common procedure and include biopsies [8], ablation probes [28], regional anesthesia [19] and brachytherapy [87] among other procedures.

Automating these procedures could increase accuracy and decrease execution time [14]. Increased accuracy could improve the medical outcome for patients. For instance in biopsy procedures it is important to acquire a tissue sample from the correct target, often a suspected malignant lesion. Sometimes the physician misses the target, in which case he or she must redo the biopsy, causing more discomfort for the patient and increasing the execution time for the procedure.

There are two main setups possible for automation of needle insertion procedures: using one robotic arm or two robotic arms. When using one arm, both the ultrasound probe and the needle-driving part are mounted on the robot end effector. One benefit of this approach is that the main parts are rigidly attached to each other, and their relative pose is known. When two robotic arms are used, one arm holds the needle while the other holds the ultrasound probe. This system is more flexible and can also handle other procedures than needle insertions.

For safety reasons, autonomous systems in health care should have a fallback solution in case anything goes wrong during the procedure. A physician should be able to operate the robots by telemanipulation and take control of the procedure in case of unanticipated and potentially harmful events.

1.1 Aims

The main aim of the thesis is to contribute to a semi-autonomous active sensing system used for tracking a needle during insertion. The objective is twofold: first, to research and develop of a robotic ultrasound image-acquisition system; secondly, to research a needle tracking algorithm using ultrasound images.

Robotic systems for acquiring ultrasound images have been researched for some time, however very few commercial systems exist. In our opinion, there is a gap between available technology and research and what is available on the market. In this thesis we to investigate whether a robotic ultrasound system can be made using commercially available components. To do this, a set of requirements for such a system must be found, and a verification that the newly created system meets all the requirements.

The second objective is to track the needle. This can be done using only ultrasound images, but it is possible that using additional sensors will increase the tracking accuracy. One important point is that the tracking of the needle must be done in real time, as the position information is needed by the robot (or person) inserting the needle. The tracking should also be robust so that it can be used with an autonomous system for needle insertion. In this thesis, 2D ultrasound images are used, which creates another challenge. For the needle to be imaged, it must be in the imaging plane of the ultrasound probe. These issues form the second line of research inquires in this thesis.

The above aims are summarized in the following points, with underlying research questions.

- Investigate whether it is feasible to make a robotic system for acquiring ultrasound images using commercially available components
  - What are the safety and system requirements for a robotic ultrasound system?
  - Is it feasible to fulfill the requirements using a commercially available robot?
  - Will the force and haptic control of such a system satisfy the requirements?
  - Do the acquired ultrasound images satisfy the requirements?
- Investigate how to track a needle using 2D ultrasound images and possibly other sensor information in real-time
  - How is it possible to efficiently track a needle in real time using only ultrasound images?
  - What are the possible gains of using sensor information from the robot?
  - How should the situations where the needle is not aligned with the ultrasound image plane be handled?

1.2 Outline

This thesis is a collection of papers and the four included research papers constitute the research contribution of the thesis. Chapter 2 reviews the relevant medical background and the state of the art of the relevant fields for this thesis. Chapter 3 accounts for the methods, materials and software used in the research, while Chapter 4 gives an overview of the research contributions of this thesis. In Chapter 5 the main findings of this thesis are discussed, and conclusions are given in Chapter 6.

Chapter 2

Background

2.1 Ultrasound-guided interventions

Percutaneous ("through the skin") access for diagnostic and treatment purposes is commonly used in modern medicine and involves inserting a thin tubular device though the skin to reach a target inside the body [4]. Possible applications include biopsies [8], ablation [28], regional anesthesia [19] and brachytherapy [87] among other procedures. These procedures are most commonly guided by one or more imaging modalities, including Ultrasound (US), Computed Tomography (CT), Magnetic Resonance Imaging (MRI), and fluoroscopy. This thesis focus on ultrasound-guided percutaneous needle insertion and this section will provide an introduction to the ultrasound imaging modality and two commonly performed procedures using ultrasound: biopsies and ablation.

2.1.1 Ultrasound as an imaging modality

In ultrasound imaging, sound waves in the frequency range of 5-10 MHz are transmitted into the body by a handheld probe. The sound waves propagate in soft tissue and are reflected due to difference in acoustic impedance within the tissues. A difference between the speed of sound in the tissues causes the reflection. Ultrasound waves do not propagate in air and bone, so these structures should be avoided for good imaging [69].

A typical medical ultrasound machine consists of a computer system, a display and a set of probes that can be easily exchanged, all mounted on a wheeled chart. The most common probes have a linear array of elements which creates a 2D image of a slice from the probe and into the tissue. Recently, 3D transducers have emerged on the market that produce 3D imaging by acquiring one 2D image at the time and combining them to construct a 3D image [69].

The US imaging modality is a real-time modality, and depending on the particular settings on the machine it will have a frame rate of 15 - 30 frames per second. Acquiring ultrasound images is also operator dependent, it highly depends on the particular skill of the clinician performing the scan [72]. The image often appears grainy as a result of speckle, which is a non-coherent reflection phenomenon, and is hard to interpret. The nature of ultrasound waves reflection may, in some cases, create artificial structures which are indeed not present in the patient's body. These objects are called artifacts, and the physician needs to be skilled in order to correctly identify and avoid artifacts.

2.1.2 Medical Ultrasound Wave Characteristics and Artifacts

An understanding of the physics behind this modality is important for interpreting the images properly. In this section we will first look at some of the physics behind ultrasound and then we will look at different types of artifacts the appear because of this.

Ultrasound waves

When ultrasound waves are sent into a body, three main phenomena occur: reflection, refraction and attenuation.

Reflection When an ultrasound beam is sent into a body, a part of the energy will be reflected back when the beam passes from a medium with one set of characteristics to another. Acoustic impedance is used to describe the tissue and enables us to quantify the reflection rate. The acoustic impedance is denoted Z and can be calculated by $Z = \rho c$, where ρ is the tissue density and c is the speed of sound in the tissue [31]. The *amplitude reflection coefficient* is given by

$$R = \frac{Z_2 - Z_1}{Z_2 + Z_1} \tag{2.1}$$

This coefficient specifies the reflection rate when a wave travels from medium 1 (Z_1) to medium 2 (Z_2). It is this effect which makes it possible to use ultrasound to generate images, but it also generates artifacts, as we shall see later.

The type of reflection ranges between scattering and specular reflections. Objects with a size of less than a tenth of the wavelength will start to vibrate when hit by an ultrasound beam. This vibration will make them a point radiation source with a spherical field. Objects that are larger, but still less than the wavelength size, will emit a non-uniform field. This is called scattering. Specular reflection is when the beam hits a perfect flat surface and is reflected according to the law of reflection, which states that the angle of incidence equals the angle of reflection [31].

Refraction As with other waves, ultrasound waves refract according to Snell's law [31]

$$\frac{\sin \theta_i}{\sin \theta_t} = \frac{c_1}{c_2} \tag{2.2}$$

where θ_i is the angle of incidence and θ_t is the angle of transmission. c_1 and c_2 represent the speed of sound of the two mediums. This phenomena can cause the target object to appear at the wrong position in the ultrasound image.

Attenuation When an ultrasound wave propagates, energy is lost in the tissue and either converted into heat or reflected back. The intensity of the ultrasound wave is reduced exponentially following the equation

$$I_x = I_0 e^{-ax} \tag{2.3}$$

where I_0 is the initial intensity, a is the attenuation coefficient and x is the distance. Attenuation is a limiting factor for how deep into the tissue one can image. For instance, for a 5 MHz probe, the depth is restricted to about 15 cm. It is worth noting that a is frequency dependent and is often modeled as

$$a = a_0|\omega|^y, \qquad 0 \leq y \leq 2 \tag{2.4}$$

in medical ultrasound where ω is the frequency component. A common rule-of-thumb is that the attenuation varies linearly with frequency with a attenuation equal to 0.5 $dB/MHz/cm$. In reality the attenuation has large variation. For instance in liver y may vary from 1.0 to 1.3, and the the attenuation constant may be between 0.35 and 0.9 $dB/MHz/cm$, while in breast tissue the exponent y be as large as 1.5 [36, 66].

Resolution

There are three types of resolutions in ultrasound imaging, axial, lateral and temporal [77]. The axial resolution (depth resolution) is frequency dependent and approximately one half of the pulse length (product of the number of cycles and the wavelength [66]). Thus, higher frequency gives higher axial resolution, but at the cost of higher attenuation. Lateral resolution is the ability to distinguish two objects lying at the same depth in the image, perpendicular to the ultrasound beams. This resolution is dependent on the distance between two transducer elements. The shorter distance, the the higher the resolution. The temporal resolution (time resolution) [66] depends on three main factors. The first factor is the frequency, which defines the penetration depth. When sending out a signal, the machine must wait for the echo; thus, the longer the waves propagate, the longer one has to wait. The second factor is the number of scan lines employed. The ultrasound image is created by sending several beams in different directions, and only one beam can be sent at a time. The last factor is the number of focal points. With beamforming the beam can be focused to a specified depth, either when sending or receiving the beam. Only one focal point can be used when sending the beam, but more several focal point can be attained using beamforming on the received signal.

Artifacts

Artifacts are defined as either missing or falsely perceived structures or degraded images in [76], which lists a large set of artifacts that might occur when using medical ultrasound imaging. A summary of a subset of these artifacts is provided below:

Overgain and undergain artifacts Setting the gain on the ultrasound machine too high or too low might obscure existing structures or cause them to disappear from the image, respectively. It is important to tune both the overall gain (i.e. the overall signal amplification) and the time gain compensation (i.e. adjustment for the sensitivity at each depth to compensate for signal loss deeper in the tissue).

Lateral resolution artifacts Most ultrasound machines can electrically focus on a given depth. If the depth parameter is set incorrectly, two objects on the same depth might appear as one single object. This type of artifacts may be avoided by setting the focus to the correct depth value. But lateral resolution is also related physical properties of the probe used. The frequency and the aperture size determines how well the ultrasound machine is able to distinguish between two objects laterally.

Acoustic shadowing This happens when a structure has a larger attenuation coefficient than the tissue beneath it, or when a structure reflects most of the ultrasound waves [76, 6] For instance, bone will reflect back (effectively blocking) the ultrasound waves, thus making the tissue underneath the bone not visible. Air and needles also causes shadowing. For needles this can be useful, for instance when inserting a needle out of the ultrasound plane; there will be a shadow beneath the needle making it easy to find the lateral position of the needle.

Acoustic enhancement This occurs when a structure has much less attenuation than the tissue around it; for instance, ultrasound waves pass relatively unattenuated in a fluid-filled cavity (cyst). This will result in a bright spot just behind the cyst.

No blood flow when it actually exists Doppler mode can be used to find blood flow in the ultrasound image. However, the velocity measured is dependent on the angle between the probe and the blood vessel by a factor of $\cos\theta$, where θ is the angle. If $\theta = 90°$, the measured blood flow is zero, even when there is blood flow. By tilting the probe a bit back and forth one can avoid this problem.

Reverberation artifacts When the ultrasound beam hits something, for instance, a biopsy needle, some of the beam will be reflected back and some will continue. The reflected beam will display the outer wall of the needle. The beam that continues will hit the inner needle wall and some of the beam will reflect back and some will continue. This will continue and some fractions of the beam will echo several times inside the needle and send a beam up to the transducer for each echo. This will create artifact needles below the real needle. This occurs mainly when the needle is perpendicular to the ultrasound beam, and the effect will be reduced by decreasing the angle between the needle and the beam. However, this will result in decreased needle visibility because fewer reflections from the needle will go back to the transducer.

Bayonet artifacts These artifacts appear when ultrasound beams pass through tissues with different speeds of sound. The result is that it takes ultrasound beams different amounts of time to return from the same depth at different locations. When calculating the depth of an object the echo return time is multiplied with the assumed ultrasound speed, and when the actual speed of the ultrasound beam varies from the assumed speed the calculated depth of an object will be slightly off. If, for instance, one is looking at an image of an in-plane needle, the needle might appear bent because of this phenomena.

Probe skin artifacts These artifacts appear when there is air between the probe and skin. As air does not conduct ultrasound (i.e. all the waves are reflected), there will be a shadow under the locations where air is present. A generous amount of ultrasound transmission gel is needed to achieve good acoustic coupling.

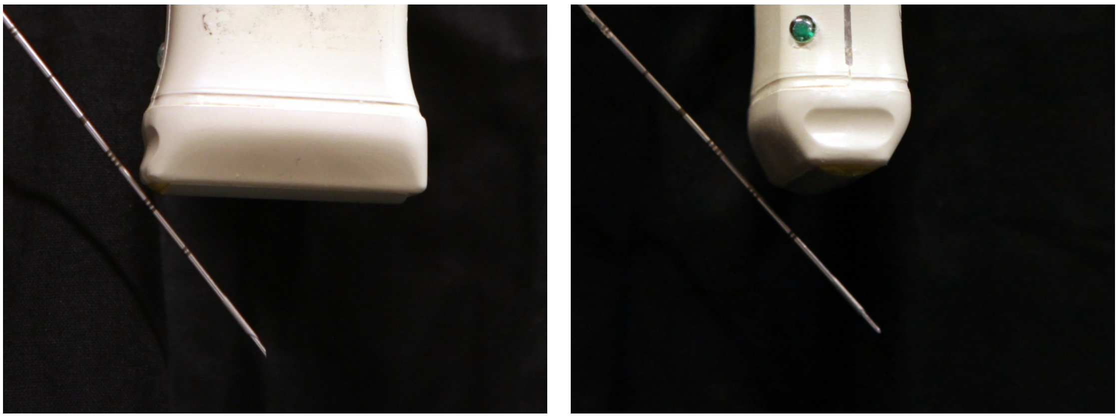

(a) (b)

Figure 2.1: Illustration of in-plane (a) and out-of-plane (b) insertion using a linear probe.

2.1.3 Percutaneous ultrasound-guided needle insertion

There are many benefits to using ultrasound compared to other imaging modalities for percutaneous needle insertion. Ultrasound is widely available in hospitals, is relatively inexpensive and is portable. Unlike CT, ultrasound does not use ionizing radiation. It also provides real-time visualization and monitoring of the needle as it is inserted into the tissue. One of the disadvantages of using ultrasound is that not all lesions can be visualized properly [8].

There are two different approaches when inserting a needle: the in-plane and the out-of-plane approach (Figure 2.1). In the in-plane approach, the needle is inserted in the same plane as the image, and the needle is visible as a bright line in the image. The advantage of this method is that both the target and needle path are visible in the image, making it easy to avoid critical regions during needle insertion. The physician may use a needle holder attached to the probe, which helps keep the needle in the image plane. Some physicians prefer to use a freehand technique when inserting the needle, allowing greater flexibility for adjustments during the insertion. In the out-of-plane approach, the needle is inserted into the image plane and appears as a bright dot in the image. Visualizing the needle tip in this approach can be difficult, as only a cross-section of the needle is imaged [19, 8].

Needle insertions are performed under sterile conditions, and the transducer is covered with a sterile plastic cover. Ultrasound gel is placed between the transducer and the cover to provide good acoustic coupling. Sterile gel is used between the patient and the cover [8].

Two common applications for percutaneous ultrasound-guided needle insertion are given below.

Biopsy

Biopsies are taken to confirm suspected malignancies or to characterize lesions in the body, and the biopsy has become an essential diagnostic technique in radiology. Biopsy needles for percutaneous biopsy can be divided into two broad categories based on their sampling mechanism: aspiration needles and cutting needles. Aspiration needles are used to obtain samples for cytologic assessment. A cytologic assessment is an analysis of the cells, and can be used for rapid testing as the pathologist can view the microscope slides just after aspiration. These aspiration needles usually have a small caliber. Cutting needles are used to obtain samples for histologic assessments. In a histologic assessment, the tissue is sampled and brought to the pathology laboratory for analysis. Cutting needles have a large caliber and are used to slice out pieces of tissue. [2, 8]

Percutaneous ultrasound-guided biopsies have many applications, and any mass that can be visualized well using ultrasound can be targeted for biopsy. This includes any superficial tissue mass, head and neck lesion, breast tumor, or solid or cystic mass in the liver, kidney, spleen, pancreas, adrenal gland or lungs.

Tumor ablation

Percutaneous ultrasound-guided tumor ablation is a minimally invasive surgical procedure used to treat malignant tumors [28]. Other imaging modalities such as Computed Tomography (CT), and Magnetic Resonance Imaging (MRI) are also used for tumor ablation [29], although US guidance is the most commonly used modality for thermal ablation [28]. A needle-shaped probe is inserted into the patient in order to destroy one or more pathological areas through the application of energy or chemicals. The advantages compared with surgical resection are the potential to destroy only a minimal amount of healthy tissue [7], lower cost [28] and faster recovery of the patient.

There are many different techniques for tumor ablation. One technique is to administer chemically ablative substances (for instance ethanol or acetic acid), which destroys the target tissue. Another technique is thermal ablation, which destroys the target tissue by either heating it or freezing it. Cryoablation probes freeze the tissue by using gas. The gas expands in a chamber at the tip of the probe and cools down the surrounding tissue. Radio Frequency (RF) probes are commonly used to heat the tissue to cause cell death. Electrical current from a generator oscillates between the electrodes, and the current flow in the tissue between the electrodes generates heat. [7]

2.2 Robotic ultrasound systems

Medical ultrasound has been coupled with robotics in many different ways. Many systems have an ultrasound probe mounted on the end effector of a robot. In this chapter we have divided these systems into two broad categories: the ones where tele-operation is one of the primary goals, presented in Section 2.2.1, and systems without teleoperation, presented in Section 2.2.2. For a comprehensive review the reader is referred to [71].

2.2.1 Telerobotic US systems

All the systems in this category are tele-manipulated and most of them are intended to be used for remote diagnostics. They are presented in no particular order, but successor projects are presented after their origin project. Table 2.1 gives an overview of the projects included in the survey. In the table, *DOF* stands for degrees of freedom of the manipulator. *Force* indicates whether the robot can be force controlled or not, *Tele* indicates that the manipulator can be telemanipulated and *Visual* indicates that a visual servoing algorithm is used on the ultrasound images. Visual servoing methods are treated separately in Section 2.3.

MIDSTEP

The MIDSTEP (Multimedia Interactive DemonStrator TElePresence) [23] is a system designed to investigate whether remote telesurgery is possible, both over LAN and WAN. A demonstrator system was created using a robot holding the ultrasound probe at the remote site. The robot is controlled by an expert at another site. An expert guides a surgeon at the remote site to perform simple invasive tasks. The motivation for the project was that few emergency units in hospitals can justify having 24-hour ultrasound services because they are only occasionally used. The project tries to address this issue by allowing a remotely located ultrasound radiologist to assist in a laparoscopic procedure or perform a telescanning intervention.

The communication link between the expert station and the remote location was 155 Mb/s for the laparoscopic system and 25 Mb/s for the telescanning system. The data flow was divided into two classes, status messages and asynchronous messages. All status messages were sent with UDP while the asynchronous messages were sent with TCP. To maintain the images streams (ultrasound, close-up video and room view) at a frame rate of 15 frames/s, the images were compressed 10:1 with JPEG and the resolution was set to 384x288.

SYRTECH

The SYRTECH project (Telescanning Robot System) [30] is a teleoperated mobile ultrasound system with a 3 DOF (roll, pitch and yaw) robot. The system is designed for use in difficult-to-access locations or remote regional medical centers. The prototype has been used in a telemedicine mission between Bourges (France) and Katmandu (Nepal).

Two main challenges were addressed when designing the system. Since the system in intended for use in difficult-to-access sites, it should be lightweight and easy to transport. The system should also be easy for an expert to use; ease of use was achieved by using a joystick to control the robot.

Table 2.1: Overview over robotic medical ultrasound projects

Name	DOF	Input	Force	Tele	Visual	Goal	Paper
MIDSTEP	-*	3-space mouse	-	√	-	Make an expert guide a surgeon at the remote site	[23]
SYRTECH	3	Joystick	-	√	-	Perform ultrasound examinations at remote difficult access locations	[30]
TERESA	4	Magnetic tracker	-	√	-	Perform ultrasound examinations in space	[79]
OTELO	6	Psaudo-haptic fictive probe	√	√	-	Perform tele-ultrasound examinations using wireless communication	[21]
ESTELE	4	Virtual probe	√	√	-	Commercial tele-echography robot	[3, 9, 15]
PROSIT	4	Hand-free haptic device	√	√	-	Create a complex robotic tele-echography diagnosis system	[16]
TER	6‡	Haptic device	√	√	-	Tele abdominal examination, in particular on follow-up on pregnant women	[82, 80, 49]
TERMI	7	Haptic device	√	√	-	Diagnosis of the venous thrombosis	[83, 81]
UBC	6	Space mouse	√	√	√	Carotid artery examinations to diagnose occlusive disease	[73, 5]
Hippocrate	6	Manual	√	-	-	Make 3D images to monitor cardiovascular disease	[70]
Ehime Uni.	7	Joystick	√	√	-	Remote diagnosis of human abdomen	[50, 51]
Montreal U.	6	Teach/replay	√	-	-	3D reconstruction of lower limb arterial vessels	[34, 35]
Tokyo Uni.	7	Haptic device	√	√	-	Tele-echography	[58, 41]
WTA-1RII	6	Joystick	-	√	√	Automatic measurement of wave intensity at the common carotid artery	[63]
WTA-2	3	Manual	√	-	-	Prevention of musculoskeletal injuries of the operator	[64]
Our system	6	GUI / Haptic device	√	√	√	Autonomously perform and monitor an ablation in the kidney	

‡ Two DOF in a cabel driven parallell robot, plus four DOF serial robot

* Information not found

TERESA

The TERESA project[79] focuses on medical ultrasound in space. The project is a continuation of the SYRTECH project presented above. The developed robotic system is a mobile 4 DOF tele-echography system weighing 3 kg. A paramedic places the ultrasound robot on the region of interest of the patient directed by the expert doctor via a video conference system. The system uses two ISDN links between the patient and the expert system. The expert doctor uses a 6 DOF magnetic tracker to control the ultrasound probe.

The project established several requirements for the system. First of all, the system must be easy to transport. Because the robot is placed on the patient, it must be lightweight; the maximum force the system will exhibit on the patient should be limited to 15 N. The mobile robot must be easy for the paramedics to handle at the remote site. At the master site, the doctor should have an input device that resembles the ultrasound probe, and the input device should detect hand movement in real time. Finally, the the connection between the two sites should reliable and be 256 kbps (two ISDN lines).

OTELO

The OTELO system [21] is a lightweight mobile tele-echography system. It is the successor of TERESA, and is the third generation of mobile tele-echography systems. The project shows that it is possible to successfully examine a patient using a wireless link with only 128 kbps bandwith, and concludes that it was feasible to use wireless communication (i.e. cellular networks) as the communication link with the technology available when the study was conducted (2004).

ESTELE

ESTELE is a commercial system for tele-echography[3]. It has a lightweight design with 4 DOF. The system is used in [9] for fetal and adult abdominal exploration in comparison with regular echography. Tele-echography examinations were nearly as medically precise as regular echography, but took more time. In [15] the system was used for biopsy procedures, where the ultrasonographer was located at the master site and the nephrologist at the patient location at the slave site, where he or she performed the biopsy.

PROSIT

The goal of the PROSIT project[16] is *to develop an interactive and complex master-slave robotic platform for a tele-echography diagnosis application*. Robosoft, the company behind the ESTELE robot, is a part of the consortium. The first prototype of the robot has been built: it is a 4 DOF mobile robot with a remote center of motion. A new hands-free haptic device has been designed. It uses inertial sensors to register the expert's hand movements. The robot is limited to exert a maximum of 20 N on the patient.

TER

The TER system [82, 80, 49] is divided into master, slave and communication subsystems. TER is a French acronym for robotic tele-echography. The transmitted ultrasound images are 640x480 8-bit images. The robotic system is generic in design, but the research focuses on abdominal examination, in particular, follow-ups on pregnant women.

The slave robot consists of two parts. The first part is a cable-driven parallel robot. Four cables are attached to a ring where the second part is mounted. The ring can be moved by adjusting the length of the cables. The second part is a 4 DOF serial robot, which can be rotated in three directions and translated downwards. A force sensor is included in the slave robot to give force measurements to the haptic device.

The communication subsystem was tested over ISDN links by experimenting on the update frequency of the real force measurements. The master haptic device has an update frequency of 1 kHz from the local model, but uses a reduced update frequency for the real measurements from the slave robot. The haptic device is a SensAble PHANToM which has 6 DOF. Since the haptic loop doesn't get new measurements at every iteration, a generic mesh is used to calculate the force between measurements. Generally, the haptic control flow needs low end-to-end latency and very low variation in latency, but does not need a high bandwidth.

Medical experts found the system to be very intuitive and the robot controllability good, based on a test with a phantom and a volunteer. There have been several tests of teleultrasound with different configurations.

The main advantages of the TER system are that it can be adapted to the body shape of the patient without a special control scheme, and that it is lightweight and compact. The accuracy of the system is limited, but this is not considered to be important in tele-echography [80].

The system has been tested clinically. In the experiment a VTHD line from France Telecom was used with a data rate of 1 Gb/s, and the master and slave stations were 1000 km apart. All patients were examined two times, once using the normal procedures and a second time using the TER system. The doctor using the TER system was not given any other input than from the TER system. The main results were that the system is comparable with ordinary examinations and that examinations take longer time using a telerobotic system.

TERMI

The TER system is a predecessor of the TERMI system (Tele-Ecografia Robotizada de los Miembros Inferiores) [81]. The idea behind the TERMI system is to make a master-slave teleoperated ultrasound system using a haptic device as input [83, 81]. The system is to be tested diagnosing venous thrombosis. The robot is divided into two parts: one part holds the probe that controls the orientation of the probe and the axial translation, which has four degrees of freedom; the second part controls the position of the probe. According to [83, 81] the fist part has already been designed, and the the second part is said to be in progress.

University of British Columbia

The University of British Columbia has created a robotic ultrasound system [73, 5] with parallelogram linkage. using a JR^3 force/torque sensor. They measured the forces and torque between the patient and the ultrasound probe while a doctor was carrying out a carotid artery examination. The maximum force measured was 6.4 N and the maximum torque was 0.7 Nm. The robot was designed to decouple the the orientation and the translation of the probe as much as possible, therefore a parallelogram linkage was chosen. The robot was counterbalanced to ensure that it would stay in place if the power was turned off. The parallelogram linkage was constructed with carbon fiber tubes and magnesium joints and weighs less than 2.4 kg including the probe and motor. The maximum force the end effector can exhibit on the patient is 15 N.

Several control schemes are discussed in [73]. The first is a master-slave control of the robot with and without force feedback, The others include shared control modes, one operator/robot controller mode and another operator/robot controller/image processor control mode. The article briefly describes a visual servo-controller that uses a normalized cross-correlation, where the best correlation between multiple frames is sought.

One of the main features of the system presented in [5] is the ability to track features in the ultrasound images in real time. The image servo control uses three of the six DOF to control the robot, leaving three DOF for the user to control. Feasibility is shown by using the Jacobian of the ultrasound image. A control law is given and it is shown that it will converge the error to zero when tracking one or more features. This control law is tested for both cases.

Two practical applications are indicated in [5]. The first is 3D ultrasound imaging. When the location of the ultrasound transducer is known the ultrasound images can be used to create a 3D image. A tool called Stradx can be used to create 3D images with a conventional 2D ultrasound machine and an Ascension Bird sensor [5]. The Star-Kalman algorithm is used to extract the contour of the pipes in the ultrasound phantom in order to create 3D images of the pipes in the phantom. This is more accurate than the Stradx approach and uses less memory. The second application is teleultrasound. 256x256 8-bit grayscale images were transmitted with a rate of at least 10 frames/s. The visual feedback delay was approximately 500 ms.

Ehime University

A parallel robot for tele-echography is described in [50]. It uses four motors to position a gimbal above the patient. The gimbal has three rotation motors, making the system a 7 DoF system. The probe is positioned in the center of the gimbal and forces applied to the imaging surface of the probe are measured by four load cells attached to the sides of the probe. The distribution of the force sensors makes it possible to find force magnitude and angle towards the probe.

The system was tested both when the operator and patient were on the same site and when tele-operated using a ISDN link. In both situations the delay was large (2 s for non tele-operation and 5 s for tele-operation), making it hard for the operator to perform the examination.

In [51] the same robot is used and the system is extended with compliance control and state machine for coordinated motion between the operator and the compliance control.

University of Tokyo

In [58] a robot with high rigidity achieved using radius guides is presented. The slave robot has 7 DoF while the master has 6 DoF. The haptic control is realized by sending force obtain by a 3-axis force sensor from the slave to the master and velocity from the master to the slave. The master is controlled by impedance control. The system was tested with the slave site being 700 km from the master site using 3 ISDN links. Round trip delay was reported to reach a maximum of 720 ms throughout the experiment. In [41] the system is extended by introducing a dynamic switching of the impedance controller's virtual viscosity depending on the task performed by the US operator.

2.2.2 Non Telerobotic US Systems

The systems presented in this section do not allow tele-manipulation. They are listed in Table 2.1 along with the other systems.

Hippocrate

The Hippocrate system [70] is designed to be used for the prevention of cardiovascular disease. Quantification of atheromatous plaques in the arteries is one factor that provides a good index of the risk of the disease. Traditional ultrasound is not able to measure this, but 3D ultrasound images are. MRI and CT are able to measure this, but these methods are costly and it will therefore be beneficial to find another method. The goal of the project is to be able to quantify the atheromatous plaques in the arteries by creating 3D images by combining 2D ultrasound images from known locations. The robot moves the probe along the artery applying a constant force of 1 to 5 N and records images at a fixed distance from each other. Each record must be synchronized with the heartbeat. If not, the result may be erroneous because the diameter of the artery varies during the cardiac cycle.

The robot used in the feasibility study was a PA-10 7 DOF robot from Mitsubishi Heavy Industry. The robot was modified to meet the requirements for safe patient interaction. A list of indispensable requirements that were used in this work is given in [22]. The external force control scheme was used citede1988compliant2.

The recording of the 2D ultrasound images requires manual initialization. The doctor can move the probe by applying force to it. The robot then transforms the force into a move command. The doctor teaches the robot a starting point and an ending point. The robot then moves automatically from the starting point to the ending point and records the 2D ultrasound images at fixed intervals.

The main goal of the project was to create an intrinsically safe robot. The Hippocrate system was developed in cooperation with Sinters. Each sub-part of the system is designed according to MIL-STD 1629A[1], which is an official safety method in the aeronautic industry. The external force on the probe is limited to approximately 30 N. The design of the Hippocrate system ensures that even if no software safety features are implemented, the system will still be intrinsically safe. The stepper motors in the robot cannot overspeed, and torque limiters have been installed. In addition several other safety features have been implemented in both software and hardware; these are listed in [70].

The Hippocrate system has a force/torque sensor from ATI Industrial Automation. The sampling rate is 10 ms and cannot be larger because of acquisition methods, but this is considered sufficient. The repeatability of the robot is 0.05 mm, the force accuracy is 0.1 N and maximum payload is 20 N. The robot was used to measure the diameter of the carotid artery. The contact force was set to 5 N and distance between records was set to 1 mm.

University of Montreal

In [34] an industrial robot from CRS Robotic Corporation is evaluated for position accuracy. The robot is used to make a 3D reconstruction of the lower limb arterial vain to quantify one or more stenoses in the vain. The robot was found to have a position accuracy of less than 0.75 mm and a repeatability of less than 0.20 mm. The system reconstructed a phantom vain with high accuracy.

WTA

Waseda Tokyo Women's Medical Aloka system (WTA) includes two robotic systems (WTA-1RII [63] and WTA-2 [64]) developed at Wasada University in Tokyo. They have different properties and both will be discussed in this section (even though one can be teleoperated) since the main focus of the project is not tele-echography.

The purpose of the WTA-1RII system is to measure the wave intensity at the common carotid artery, which is an index used to detect cardiovascular changes. It is a 6 DoF master-slave system that can be controlled by a robot. An automatic method to find to optimal view of the carotid artery is also implemented and tested. This method maps a region and analyses the US images to find the optimal view. The user only has to provide the starting point for the examination.

WTA-2 has a different purpose than its predecessor. The main focus is the prevention of musculoskeletal injuries to the operator, and a 3 DoF robot with changeable tool has been developed for this purpose. One tool holds a US probe, which the operator can move by simply holding it; sonographers reported that it was difficult to handle the probe using a master-slave setup. Photo sensors were attached to the probe to detect the forces applied by the operator; having the force sensor between the robot and the probe makes it impossible to differentiate between the forces applied by the operator and forces from contact with the patient. A usability study showed that the system was hard to use for the sonographers, as they had a difficulty understanding the level of applied force.

2.3 Needle tracking in US images

Needle tracking in US images can be divided into two different categories depending on whether a 2D or 3D probe is used. Some methods involve visual servoing of the US probe based on the needle in the image. These methods are presented in Section 2.4.

2.3.1 Tracking in 2D images

A needle localization method for ultrasound-guided breast biopsies is presented in [27]. The method involves finding a variance image using an 11x11 kernel and thresholding this image. A principal component analysis was performed to find a set of possible needle candidates, and the needle with the large variance in the direction of the major axis was chosen. Experiments were conducted using an agar phantom, and the results from the method were compared with manual segmentation.

A real-time algorithm for finding straight biopsy needles is presented in [25] based on a modified version of the Hough transform. The main modification of the transform is to use a coarse-fine search strategy to achieve real-time execution. The method thresholds the US image before applying the modified Hough transform to find the needle orientation and axis. The needle tip is found by searching the axis from the entry point and ignoring small gaps along the line. Experiments were conducted on five agar phantoms and one patient biopsy. The results showed an RMS position error on the order of 0.5 mm.

In [68] two real-time algorithms for finding curved needles in 2D US images are presented, one based on the Hough transform and one approximating the curved needle as an arc of constant radius. The algorithms find points on the needle, but do not provide a reliable estimation of the needle tip position.

Those algorithms are compared with a novel method for finding biopsy needles on transrectal ultrasound (TRUS) images where both of the above algorithms are found to give biased results in [20]. The algorithm in [20] defines an objective function from three needle tip metrics and selects the needle tip based on this function. The results are very accurate, but all the images of the biopsy procedure need to be available prior to the execution of the algorithm. Therefore the method is not suitable for real-time applications.

In [10] a biopsy needle segmentation method is presented, also for TRUS images. The method uses a second derivative of Gaussian filter to enhance the tubular structure of the needle. The TRUS video stream is then analyzed to find the image containing the needle. This is necessary because the biopsy needle is fired into the patient and only stays there for a very short time. The objective is to detect where the needle has been, rather than to track it. When the right image is detected, it is segmented using graph-cuts.

A Gabor filter is used in [38] to localize the needle, and is improved in [37] by the introduction of an entropy-based parameter tuning scheme. In addition to Gabor filtering, a median filter and Otsu's thresholding method are used. The thresholded image is processed using morphological operations and then a random sample consensus (RANSAC) method is used to estimate the needle position. Finally, the tip is estimated heuristically. The method was tested using agar, gelatin agar and gelatin and water phantoms. In [39] the method was further expanded using a Kalman filter.

2.3.2 Tracking in 3D volumes

In [12] a method for automatically localizing curvilinear objects in 3D US images is presented. The image is thresholded using a heuristically found threshold. The randomized RANSAC method is used to find the needle, modeling the needle as a three-dimensional cubic curve. Least square fitting is used on the voxels returned by the RANSAC method. The method was verified using a phantom, but no quantitative data on accuracy were given.

A method for segmenting and tracking a brachytherapy needle in 3D TRUS images is presented in [87]. A volume scan is obtained prior to insertion of the needle, and a difference image is calculated upon insertion of the needle. The image is then thresholded and small voxel clusters are removed. The remaining voxels are fitted to a line using linear regression, and the needle tip is estimated as the voxel that is furthest away from the needle entry point along the estimated line. The method was evaluated on an agar phantom.

A method for tracking a surgical tool is presented in [67]. Surgical tools have very similar image features to needles, and the method is included here for completeness. The Radeon transform is used to find a line, defined by six parameters, that corresponds to the surgical tool. A passive marker at the tip of the surgical tool is used to find the remaining two degrees of freedom (tip position and roll angle). The method was implemented in GPU for real-time execution. The experiment was conducted in a water tank and in an in vivo porcine heart. Electromagnetic tracking was used to determine the ground truth position.

In [65] the generalized Radeon transform is used to estimate the needle axis, and the axis was represented as a Bézier polynomial. The method is implemented to run at the GPU for real-time execution, using the NVIDIA CUDA framework. The accuracy of the method is checked using an agar phantom, and compared to tracking from a magnetic tracker. Processing the two first volumes is slow, and the GPU implementation uses up to 8.7 s while the CPU implementation uses up to 72.2 s. After the two first volumes the processing time is down to a maximum of 69 ms for the GPU and 1.7 s for the CPU.

Another use of the RANSAC method is presented in [78]. Here the image is first thresholded, then the axis is estimated using the RANSAC method. The axis estimate is refined using a local optimization step based on the result of the RANSAC method. The tip is identified by a significant drop in voxel intensity. The method was tested in simulations and using a polyvinyl alcohol cryogel phantom, turkey breast and patient breast biopsy.

In [90] a method for tracking biopsy needles is presented. It first introduces a strategy for automatically finding the region of interest, then the RANSAC algorithm is used together with the Kalman filter algorithm to track the needle. The method was verified by inserting a biopsy needle in a water-bathed lamb heart.

2.4 Visual servoing of US probe

One of the first reported visual servoing controls of a US probe was in [5] where a US probe was mounted on a specially made robotic system, already mentioned in Section 2.2.1. A carotid artery was tracked using five different techniques, which were cross correlation, sequential similarity detection, edge detection (Star algorithm), Star algorithm with Kalman filter and active contour (Snake algorithm). The robot was controlled in 3 degrees of freedom (DoF) using visual feedback, and the Star-Kalman algorithm was found to have the best tracking performance. One application for the reported visual servoing method is 3D reconstruction of arteries and veins.

IRISA, INRIA Rennes-Bretagne Atlantique in France has made extensive contributions to the visual servoing of US probes. In [11] visual servoing of 2D images is performed on an egg-shaped object where the robot moves the probe in 6 DoF to view a specific cross-section of the egg shaped object. This shape is common in tumors and the method could be used to hold a specific view of a tumor. A drawback of this method is that it requires a pre-operative model of the tumor. Simulations show that the the visual feature errors converge towards zero, and that the method is robust against noise and initial modeling errors.

In [56] image moments are used as visual features to implement the control law, and both in-plane and out-of-plane motions are addressed. The method was tested in simulations and using a robot. However, only egg-shaped objects were considered in the paper, an issue that is addressed in [57]. The method is now model-free, and the approach has been improved and broadened. The method was validated using a simulation, on a US phantom and on a ex-vivo lamb kidney. In [55] further improvements are made to the online feature estimator.

A method for stabilizing the probe at one view, even if the patient is moving, is proposed in [44, 43]. Here speckle information is used to track both out-of-plane and in-plane motion of the probe. This is possible because speckle is not white noise, but rather highly correlated over small motions of the probe. A speckle decorrelation technique is used to estimate the out-of-plane distance between images, thereby enabling the estimation of patient motion.

In [61] image intensity is used directly to control the probe to track a specific organ by compensating for rigid motion. The main benefit of this approach is that it avoids segmentation of the image. Both in-plane and out-of-plane motions are considered and simulation and experimentation on abdominal phantoms shows the validity of the method.

The tip of a flexible needle is tracked in [85] by having the US plane perpendicular to the needle. The visual servoing tracks the needle tip by moving the probe 2 DoF, always keeping the tip in the image. Experiments are performed using a phantom made of water, gelatin powder and silica gel, and the experimental results show sub-millimeter accuracy. A major drawback of this approach is that the forbidden regions are not imaged.

In [60] a multi-plane visual servoing approach is presented. The approach uses three orthogonal 2D planes, and two image moments for each plane are used as visual features. These two image moments are center of mass and orientation. The image moments for one plane represent in-plane motion for that plane, but they are coupled with the out-of-plane motion for the other two planes. Thus the out-of-plane motion is controlled by using the in-plane motion of another plane, effectively controlling the robot in 6 DoF. In practice, a small intraoperative zone is scanned and a volume is reconstructed, prior to the visual servoing. When performing visual servoing, one probe is used while the other two planes are estimated using the model.

A surgical instrument is controlled using visual servoing in [84]. The instrument is observed using an ultrasound probe, and is one of the few eye-to-hand configurations reported for visual serving using ultrasound images. The instrument is inserted into the heart through a trocar, and this reduces the degrees of freedom to four. The effectiveness of the method was verified both with simulations and in an in vivo experiment with a pig.

A visual servoing scheme for improving the treatment of kidney stones (lithotripsy) is presented in [45]. High intensity focused ultrasound (HIFU) is used to destroy the kidney stone, and the visual servoing scheme aims at compensating for movement due to respiration and heartbeat using 3 DoF. Two ultrasound transducers are mounted on the HIFU unit with perpendicular image planes. The visual servoing method is successfully used in an experiment using a model of the kidney stone, where the kidney stone has an oscillatory motion provided by a motor-driven piston. The tracking error was found to be less than 0.4 mm.

In [17] a visual control method using a 3D probe is described. The method detects the needle from the moment it is inserted, without any prior knowledge of insertion direction. It combines the random sample consensus (RANSAC) algorithm with Kalman filtering to achieve robust real-time tracking of the needle. Then the probe is then controlled in 3 DoF using the horizontal position of the needle tip and the angle between the probe's x-axis and the principal direction of the needle. Experiments were conducted on a homemade agar phantom, and the feature error converges in the experiment.

An overview of the visual servoing methods is presented in Table 2.2.

Table 2.2: State-of-the-art visual servoing control schemes

First author	Pub. date	Probe	DOF	Configuration	Features	Target	Ref.
C. Nadeau	2011	2D	6	eye-in-hand	Image intensity	Target image	[61]
A. Krupa	2007-2009	2D	6	eye-in-hand	Speckle information	Target image	[44, 43]
R. Mebarki	2008-2010	2D	6	eye-in-hand	Image moments	Target image moments	[56, 57, 55]
W. Bachta	2006	2D	6	eye-in-hand	Object contour	Egg shaped object cross-section	[11]
C. Nadeau	2010	3D	6	eye-in-hand	Object contour	Egg shaped object cross-section	[60]
P. Chatelain	2013	3D	3	eye-in-hand	RANSAC and Kalman filter	Needle	[17]
P. Abolmaesumi	2002	2D	3	eye-in-hand	Image sub block/Active contour	Carotid artery	[5]
G. J. Vrooijink	2013	2D	2	eye-in-hand	Segmented needle	Needle tip	[85]
M. Vitrani	2007	2D	4	eye-to-hand	Points in a surgical tool	3D position of surgical tool	[84]
D. Lee	2007	2x2D	3	eye-in-hand	Correlation (B-mode)/ image moments (RF)	Image of kidney stone	[45]

2.5 Needle placement robots

There are many projects involving robotic needle insertion, and this section provides a short introduction to some of the systems. A more complete overview can be found in [71].

A system for inserting a biopsy needle targeting the gallbladder is reported in [32, 33]. This work spans several different topics, but is included under the needle placement robot heading, as this its main focus. A robotic system was developed with a needle insertion robot with 2 DoF mounted on an ultrasound probe. The probe itself was mounted on a 5 DoF passive arm. The system recognizes the gallbladder using a motion-optimized active contour model, and uses the Hough transform to detect the needle. The needle is controlled by visual servoing to compensate for the movement of the gallbladder. The system was verified by an experiment using a phantom. An in vivo experiment with a pig was also performed, and the pig's breath was held when the needle was inserted. In addition, the gallbladder tracking was verified using the video stream obtained from an examination of the gallbladders of two male volunteers.

In [47, 46, 48] a novel approach for biopsies of breasts is presented. Rather than adjusting the path of the biopsy needle, the breast itself is manipulated to move the target into the needle path. The system consists of three robotic subsystems. The first is the breast manipulation system consists of three fingers that pushes on the breast, thereby moving the target inside the breast. The second subsystem is the ultrasound holding robot, which has two active DoF. The last subsystem is the needle insertion robot, which has one active DoF. Experiments with the system were carried out on a phantom breast model, and the maximum RMS error for the experiments was 0.4 mm. The error was defined as the difference between the needle tip and the target.

A system for needle ultrasound-guided robotic needle placement is presented in [13]. The target area for needle insertion is scanned with a 2D ultrasound probe that is tracked with a magnetic tracker. The area is reconstructed to a 3D volume. The needle path is planned in using an interactive 3D Slicer interface, and the robot is then positioned at the correct insertion point. The needle is manually inserted using the guide on the robot. Fluoroscopy from a C-arm was used to quantify the insertion accuracy of the procedure. The system was tested on ex vivo bovine liver and on an in vivo porcine model. In the experiments the system was compared to the traditional approach of manually inserting the needle using US guidance.

A robot-assisted approach to transrectal ultrasound (TRUS) guided brachytherapy is presented in [88]. A commercial robot is used as a movable needle guide, and the needle is inserted manually by a physician. The system uses a novel 3D TRUS system, which reconstructs 2D TRUS images. The ultrasound probe is rotated to scan a given volume. A software framework for 3D visualization and path planning was developed, and calibration and registration between the devices provides the robot holding the guide with the correct position based on the planning. Several experiments were conducted to quantify the accuracy of the different subsystems and the system as a whole.

An autonomous robotic system for needle insertion is presented in [59]. The paper is based on research carried out in the EU's Intelligent Surgical Robotics project. A novel robotic platform was developed based on a macro/micro unit architecture. This robot inserts the needle while a UR5 robot from Universal Robots holds the ultrasound probe. The paper presents a preliminary experiment on autonomous needle insertion on a phantom.

Chapter 3

Materials, Methods and Software

This chapter presents the materials used in the experiments, the methods used to analyze the results and the software used to perform the experiments.

3.1 Materials

3.1.1 Devices

The robotic system used in the thesis is a UR5 from Universal Robots, and is shown in Figure 3.1. It is classified as a collaborative robot according to EN ISO 10218-1:2006 [1]. This means that no safety guards between humans and the robot are required as long as a proper risk assessment is performed, and this makes it possible to use the robot for medical applications. The built-in safety mechanisms include stopping when the robot joint torque deviates from the expected torque, a safety stop when the external force exceeds 150 N, and an emergency stop button. The robot is also lightweight at only 18 kg. The robot has 6 DoF and can have a payload of up to 5 kg. It has a reach radius of 0.85 m and a repeatability of 0.1 mm.

A Gamma SI-65-5 from ATI Industrial Automation, which is a six degree of freedom force/torque sensor, is used to measure the forces and torques at the end effector of the UR5 robot. The sensor has a dynamic range of 65 N (F_x, F_y), 200 N (F_z) and 5 Nm (τ). The resolution is 1/80 N (F_x, F_y), 1/40 N (F_z) and 10/13333 Nm (τ). The sensor is connected to a DAQ unit from National Instruments.

The frame grabber used to acquire ultrasound images is a VGA2Ethernet device from Epiphan. The device converts VGA and DVI signals and transmits them over gigabit Ethernet.

Two different ultrasound systems have been used, a Sonix MDP ultrasound device, manufactured by Ultrasonix, and System Five, manufactured by GE. When using the Sonix MDP system, the images were obtained directly from the machine using the Sonix API. The frame grabber described above was used to acquire images from the System Five machine.

A Phantom Omni from SensAble Technologies is used for the haptic control of the robot, and is connected to the control computer (same computer as the robot) using FireWire. This device has 3 active DOF and 3 passive DOF.

[1] Robots for industrial environments – Safety requirements – Part 1: Robot

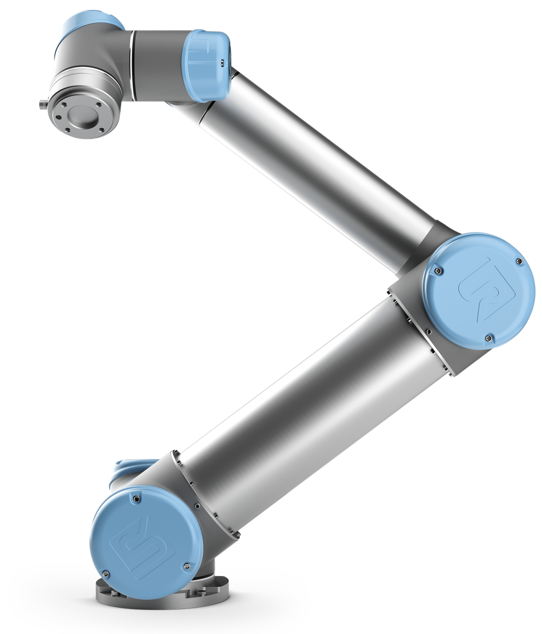

Figure 3.1: The industrial robot UR5. (Printed with permission from Universal Robots A/S.)

An Optitrack infrared tracking system from NaturalPoint was used in the experiments. The system is able to track a 3D object with sub-millimeter accuracy.

3.1.2 US phantoms

Three different US phantoms have been used in this thesis: a water tank phantom, a corn flour phantom and ex vivo muscle tissue. The water in the water tank is able to propagate ultrasound waves with speed similar to tissue, thus creating a correct image. Using water as a medium differs in several ways from using tissue. There is very little noise in the image, as there are no small particles to create this noise. Therefore, the image created in water is usually black. Another difference is that water has very little attenuation; this might lead to artifacts as the ultrasound waves are reflected on the tank bottom or sides.

The corn flour phantom is better at mimicking the properties of tissue, as the flour reflects ultrasound waves and yields similar noise characteristics as tissue. One difference from tissue is that the corn flour creates a more uniform image, without any structures. An advantage of corn flour is that it is cheap and can be used to create phantoms of an arbitrary size.

The ex-vivo muscle tissue phantom from animals closely resembles the tissue from humans, and is excellent for obtaining realistic images. It contains muscle structures, but no organs are present. This phantom also creates uniform images, although to a lesser extent than the corn flour phantom.

3.2 Methods

The work presented in this thesis primarily focuses on creating new methods for achieving the aims of the thesis. These new methods are covered in Chapter 4, rather than in this section, as they are the main research contribution of the thesis.

3.2.1 Statistical analysis

A hypothesis test is used in statistics to check if the observed difference between two population parameters is an actual difference with a certain probability. For instance, when comparing two methods, it is useful to check if the mean error is different for each of the two methods, but also if the standard deviations of the errors are different.

The t-test is used to test for significant differences between one mean and a fixed value or between two means [86]. The theory presented below assumes that both populations are normally distributed with unknown variance. With one mean the two-sided hypothesis is

$$H_0 : \ \mu = \mu_0 \tag{3.1}$$
$$H_1 : \ \mu \neq \mu_0 \tag{3.2}$$

where μ is the mean of the population and μ_0 is the expected mean. H_0 is rejected at a significance level of α if the computed t-statistic

$$t = \frac{\bar{x} - \mu_0}{s/\sqrt{(n)}} \tag{3.3}$$

exceeds $t_{\alpha/2,n-1}$ or is less than $-t_{\alpha/2,n-1}$. $\bar{x}$ is the estimated mean and s is the estimated standard deviation of the population. n is the sample size. $t_{\alpha/2,n-1}$ is the critical value of the Student's t-distribution where $n-1$ is the degrees of freedom and $\alpha/2$ is the probability value. The comparison of two means is not used in this thesis and is therefore omitted. The above t-test is used to check if the methods produce a biased result, i.e. $\mu_0 = 0$. If the null hypothesis is rejected the method have a biased result.

For comparing two variances the f-test is used. The two-sided hypothesis

$$H_0 : \ s_1^2 = s_2^2 \tag{3.4}$$
$$H_1 : \ s_1^2 \neq s_2^2 \tag{3.5}$$

is used, where s_1 and s_2 are the standard deviation of the two distributions. The test statistic

$$f = \frac{s_1^2}{s_2^2} \tag{3.6}$$

is calculated, and the null hypothesis is rejected if f falls outside

$$f_{\alpha/2}[n_1 - 1, n_2 - 1] < f < f_{1-\alpha/2}[n_1 - 1, n_2 - 1] \tag{3.7}$$

where $f_{\alpha/2}[n_1 - 1, n_2 - 1]$ and $f_{1-\alpha/2}[n_1 - 1, n_2 - 1]$ is the critical values of the F-distribution having $n_1 - 1$ and $n_2 - 1$ degrees of freedom.

A percentile is a measure in statistics that indicates the value below which a given percentage of all observations falls. For instance, the 50th percentile is the value below which 50 % of the observations may be found. The 50th percentile is also known as the median, and the 25th and

75th percentile are known as the first and third quartiles, respectively. Percentile is a useful measure if the observations are not normally distributed, and is commonly visualized in a box-and-whisker plot.

3.3 Software

Xenomai is a real-time framework for Linux. It uses a dual kernel configuration, where the real-time tasks run in one domain and the Linux kernel and programs run in another domain with lower priority. All interrupts are first delivered to the real-time domain to check whether a task in that domain will handle the interrupt. The interrupt is then delivered to the Linux domain when no real-time tasks are scheduled. The framework makes it possible to run hard real-time tasks on a Linux system.

OpenCV is a computer vision and machine learning library available on many platforms and programming languages. It is an extensive library with a comprehensive set of both classic and state-of-the-art computer vision and machine learning algorithms.

Armadillo Linear Algebra [74] is a linear algebra library for C++ which uses similar syntax to Matlab. It is wrapper library using functions from LAPACK, BLAS and ATLAS, which all are linear algebra libraries.

A software framework for controlling the UR5 robot and logging experimental data was developed as a part of this thesis. We consider this a research contribution and the framework is briefly described in Chapter 4 under Paper I.

Chapter 4

Research contribution

The main aim of this thesis is to contribute to a sensing system for tracking a needle as it is autonomously inserted by a robot, and each paper contributes in different ways to this goal. The relationship between the different papers is illustrated in Figure 4.1. In Paper I, a robotic ultrasound system with both force and haptic control is developed. The system is designed to hold the US probe and acquire ultrasound images of the needle while it is being inserted. Papers II and III address the tracking of the needle. In Paper II, the needle is inserted manually and tracked using US images. In Paper III, the needle is inserted using the robotic system from Paper I and the US probe is held by a passive arm. Both imaging and robot velocity are used to estimate the needle position. One issue that became apparent when performing experiments for Papers II and III was that the alignment of the US probe and needle was crucial for good visualization of the needle in the US image. Even with accurate registration and an optical tracking system the needle could be inserted with an angle to the image plane, thus resulting in poor needle visualization. This led to the development of a visual servoing method, presented in Paper IV, for aligning the needle and image plane. Table 4.1 gives an overview of all the papers, while each paper will be summarized more thoroughly in the subsequent sections.

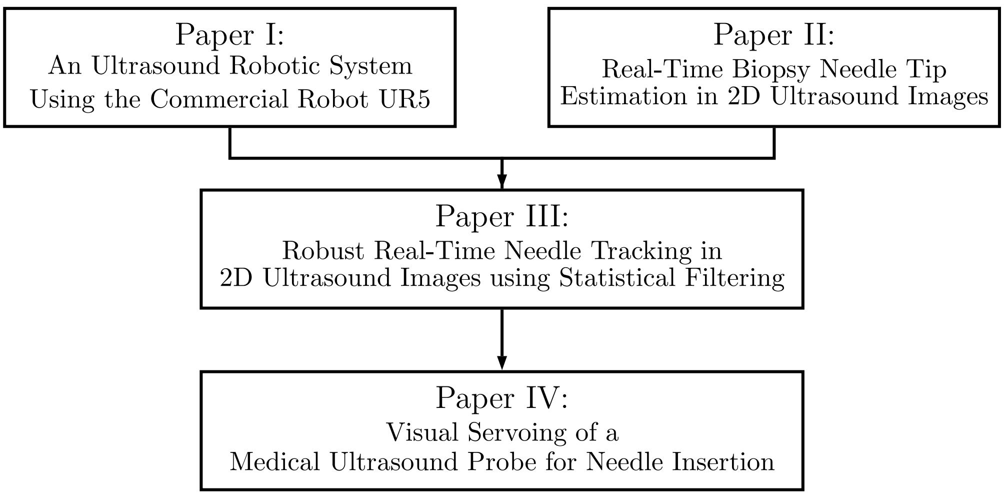

Figure 4.1: Diagram describing the relation between the papers in the thesis.

Table 4.1: Overview of the aims, methods and results of the papers included in the thesis

Paper	Aim	Methods	Result
I	• Investigate the feasibility of using an collaborative industrial robot to develop a robotic ultrasound system • Develop a robotic ultrasound system with force and haptic control	• Analysis of robot workspace • Compliance force control • Forward flow haptic control	• A robotic ultrasound system the collaborative industrial robot UR5 • A software framework for controlling the UR5 robot and logging experimental data
II	• Accurately track a needle in a US image in real-time	• Method in [68] used to estimate needle axis • Two novel image filters • Five features are used to extract the needle tip position	• Mean tracking error of 1.73 mm • Maximal execution time of 19.21 ms
III	• Improve the robustness of the tracking in Paper II	• Dynamic ROI • Kalman filter and particle filter are used to remove outliers and filter out noise • Method may use insertion velocity from a robot for increased estimation accuracy	• Mean tracking error of 0.82 mm using both US images and robot velocity and 1.68 mm when only using US images • Maximal execution time of 28.23 ms
IV	• Align US imaging plane to a needle using visual servoing	• Needle segmentation using two filters • Image moments used to extract visual features • Kalman filter used to filter noise from the visual features • State machine selecting visual features based on needle position/state	• Simulation shows that the method behaves as intended • An experiment shows that the method manages to align the image plane to the needle

4.1 Paper I

Medical ultrasound is an important image modality in diagnostics and treatment in modern medicine and is used extensively in cardiovascular imaging [69] and fetal screening examinations. Other diagnostic procedures include ultrasound-guided biopsy, which is an essential diagnostic technique in radiology [8].

Ultrasonography is highly operator-dependent [72], and it is therefore important to have a skilled physician performing the procedure. As the use of ultrasound is becoming more common, local physicians might want to ask experienced physicians for assistance during a consultation. Having a teleoperated ultrasound system would enable the experienced physician to take control of the probe and assist the local physician. The main contribution of this paper is to examine the feasibility of using a collaborative industrial robot for a teleoperated robotic ultrasound system. Unlike industrial robots used in other research in this area, the robot used in this study has built-in safety features, which means that it will be conducive to safe human–robot interaction. A secondary goal of this research is to develop a system for acquiring ultrasound images for autonomous needle insertion.

The paper derives a set of requirements for an ultrasound robotic system based on state-of-the-art systems and divides the platform development into three parts, as in Courreges et al. (2008):

- Slave site: Location of the patient, the robot, ultrasound machine, and medical staff to monitor the procedure.
- Communication link: The data link and protocols used between the two sites.
- Master site: Location of the physician, who controls the robot and views the ultrasound images.

Quantitative requirements for these parts are found. The master site has a haptic device that controls the slave robot.

A novel system is developed in the paper using the collaborative industrial robot UR5 from Universal Robots. A Gamma SI-65-5 from ATI Industrial Automation six degree of freedom force/torque sensor is mounted on the robot end effector and the US probe from a GE System Five is mounted on the force sensor. The UR5 with force/torque sensor and attached US probe is used as the slave robot. The master robot is a Phantom Omni from SensAble, which has 3 active DOF and 3 passive DOF. The developed system is shown in Figure 4.2.

The controller of the two robots runs a Linux system using the real-time extension Xenomai. A complete framework for interface and controlling the robot was developed using low level interface of the robot. Compliance force control [75] and forward flow haptic control [62] were implemented, along with kinematics, software safety mechanisms and a LabVIEW-based graphical user interface.

Three different experiments were conducted. The first experiment checked the real-time properties of the control systems. The second and third experiments were designed to determine the characteristics of the force control and the haptic control, respectively.

The experiments show that the real-time properties are met, except for the frame rate of the US machine, which was 23.9 fps. The force control met all the requirements and had a

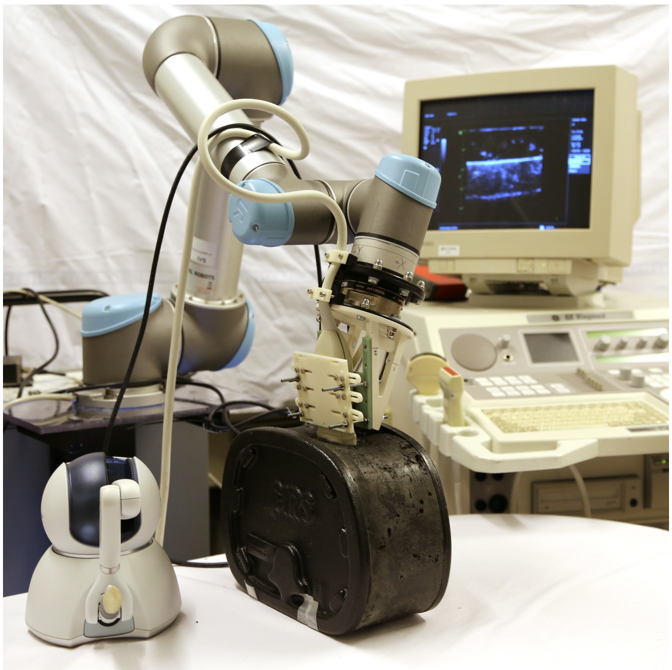

Figure 4.2: The developed robotic ultrasound system from Paper I.

bandwidth of 16.6 Hz. The forward flow haptic control was unable to have a control frequency of 1000 Hz, and it was lowered to 700 Hz. The bandwidth of the position and force control in the haptic loop was 65.4 Hz and 13.4 Hz, respectively, thus meeting all the requirements.

4.2 Paper II

Ultrasound-guided biopsy is a safe and accurate method for verifying the malignancy of a tumor [8]. Automating this task using a robot could increase accuracy and decrease execution time [14]. When automating, it is important to know the position of the needle and the direction it is traveling inside the body while the robot is inserting the needle. This paper addresses this issue by estimating the position of the needle tip along with the insertion angle of the needle directly from the US images.

The main innovations in the paper are two image filters for enhancing the needle in the ultrasound image, and a set of five features for finding the needle. The developed method can be executed in real-time and is accurately evaluated using an optical tracking system.

The method proposed in the paper is divided into two steps. In the first step, the needle insertion angle is estimated using the method in [68]. The second step involves finding the needle tip along the needle axis (found in the first step).

First, two filters are applied to the image. The graylevel US image is shown in Figure 4.3(a). The first filter is based on a square kernel and the filtered image is shown in Figure 4.3(c). Red indicates a positive value, blue a negative value and white is zero. The second filter has a kernel based on the second derivative of a Gaussian, and the filtered image is shown in Figure 4.3(d).

All five features are based on estimating the derivative of the pixel values along the needle. A high derivative value indicates a sudden drop in pixel value and indicates that the needle might end there. The images used for finding the five features are given in Figure 4.3. Figure

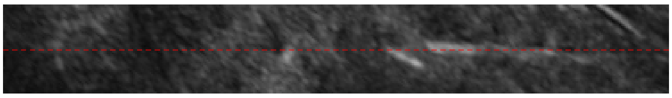

(a) I^{GS}

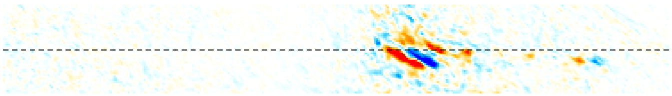

(b) I^{Δ}

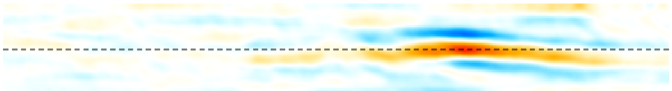

(c) I^{SQ}

(d) $I^{G''}$

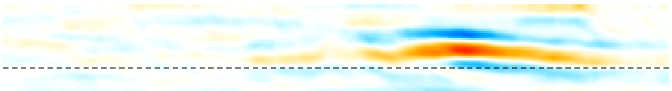

(e) I^{SQ} with offset

Figure 4.3: The features are calculated from the grayscale US image (a) along the dotted line representing the needle axis. In (b)-(e) blue represents negative values and red positive.

4.3(b) is a difference image between the current image and an image 10 frames ago. The last feature, from Figure 4.3(e), is using the image obtained with the square kernel, but with an offset. The features are combined using the linear function

$$h(x) = \sum_i w_i E_i(x) \tag{4.1}$$

where w_i if the weighting of the ith feature, E_i is the ith feature value of the position x along the needle. The maximum of $h(x)$ is selected as the needle tip position.

Two experiments were conducted by manually inserting a biopsy needle into a phantom. The insertion was imaged using an US probe, and both the probe and needle were tracked using an optical tracking system. The rigid transformation between the probe and needle was found in order to map the needle orientation and tip position into the image. These values were used as a gold standard for comparison with the proposed method in the paper. Six insertions were made into a phantom made from a mixture of corn flour and water and eight into an ex vivo pig muscle sample. These experiments are divided into two datasets, denoted 1 and 2, by taking half of insertions in each phantom. One dataset trains the wights in $h(x)$, while the other is used to find the errors of the method.

Dataset 1 has a mean position error of 1.57 mm with a standard deviation of 2.20 mm and the 95th percentile of the error is 3.49 mm. For dataset 2 these values are 1.73 mm, 2.37 mm and 4.02 mm. The maximum execution time for one image was 19.21 ms.

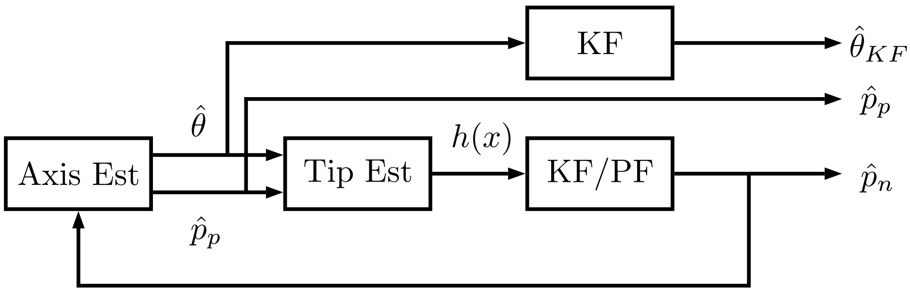

Figure 4.4: An overview of the method presented in Paper III. "Axis est." is the axis estimation with estimates the needle insertion angle $\hat{\theta}$ and the needle entry point $\hat{p}_p$. "Tip est." is the tip estimation from Paper II. "KF" is a Kalman filter that filters the estimated insertion angle $\hat{\theta}$. "KF/PF" is either a Kalman filter or a particle filter estimating the needle tip position along the needle axis $\hat{p}_n$.

4.3 Paper III

This paper address the same issue as Paper II, but improves the method in several ways:

1. on-line adaptation of the region of interest for estimating the needle axis in a more robust and reliable way,

2. implementation of statistical filtering: Kalman and Particle filters have been used to improve the accuracy and precision of the tip tracking, to filter out the noise, and to cope with outliers,

3. the algorithm can also rely on velocity measurements to improve the tracking accuracy when the insertion is performed by a robotic system.

Two other major differences with Paper II are that the needle was inserted by a robot and a physician manually found the gold standard for needle position and orientation, rather than using an optical tracking system.

An overview of the method presented in this paper is shown in Figure 4.4. The method starts by estimating the needle insertion angle and entry point. The method in [68] is improved by introducing a dynamically adapting region of interest around the needle. The insertion angle is filtered by a Kalman filter to reduce the noise of the estimate.

After the needle axis is found, $h(x)$ is calculated as in Paper II ("Tip est" block in Figure 4.4). The result is used as a measurement update in either a Kalman filter or a particle filter. In the case of the Kalman filter, Bayesian theory is used to select the most probable needle tip position, based on both $h(x)$ and the current tip position estimate. The variance of the measurement varies and depends on the probability of the selected tip position. In the case of the particle filter, a prior is created using $h(x)$ and the current estimate of the tip position.

Because the needle is inserted by a robot, another measurement can be included. Both the Kalman filter and particle filter are expanded to include the robot velocity when estimating the needle tip position, which improves the tracking performance.

The experimental setup includes a UR5 robot, which inserts a biopsy needle into a beef phantom. The insertion is monitored using an US probe. An optical tracking system is used

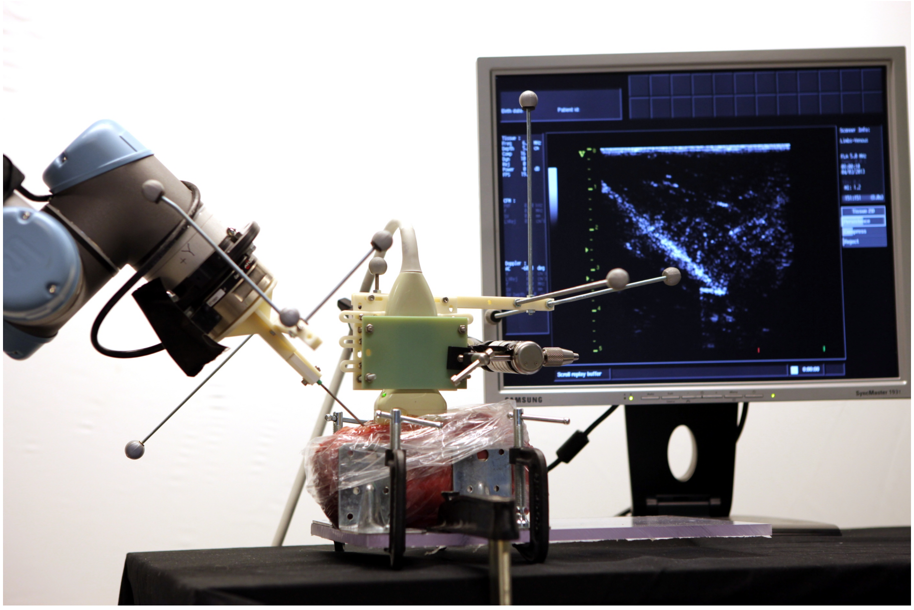

Figure 4.5: The experiment setup in Paper III, consisting of a UR5 robot (Universal Robots) for inserting the needle, an ex vivo meat phantom, a System Five ultrasound machine (GE Vingmed) and a OptiTrack infra-red tracking system (Natural Point Inc.) for aiding the robotic insertion.

to align the needle and US image plane. The experimental setup is shown in Figure 4.5. Two experiments are conducted, one for training and one for validation. The training experiment has six insertions, while the validation experiment has 18 insertions. A physician manually marked the needle insertion angle and tip position in the images. The values were treated as the gold standard, and compared with the results from the presented methods.

Table 4.2: Main results of Paper III, showing the tracking error of different methods. DF is the method presented in [25], OM is the method presented in Paper II. KF+F is using Kalman filter and dynamic ROI and KF_v+F is additionally using robot velocity measurements. Std is the standard deviation and PCTL stands for percentile.

Methods	Error [mm]		
	Mean	Std.	95th PCTL
DF	13.75	10.09	33.68
OM	3.55	6.23	17.21
KF+F	1.68	1.72	5.54
KF_v+F	0.82	0.76	2.17

The methods presented in this paper were compared to the method in Paper II and the method in [25]. The main results are presented in Table 4.2. Other novel methods were tested in the paper, for instance using the particle filter, but only the two highest performing methods are shown here. The maximum execution time is 28.23 ms.

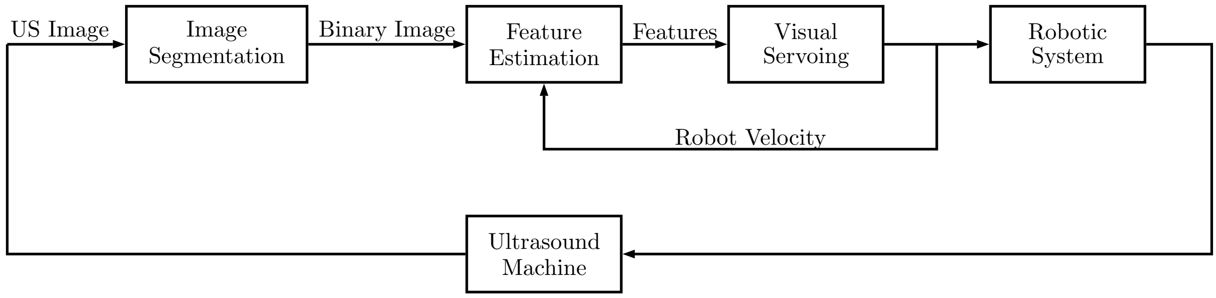

Figure 4.6: An overview of the visual servoing control loop from Paper IV.

4.4 Paper IV

One issue with the methods presented in Papers II and III is that the needle must lie in the imaging plane of the US probe. This paper address this issue by presenting a novel visual servoing scheme by using image moments, Kalman filter, visual servoing theory and a state machine to select visual features depending on the needle orientation/state. The method was tested using simulation and experiments. The control approach is the main topic of the paper, therefore a water tank is used as a phantom in the experiment to simplify the segmentation of the needle. The main contributions in the control approach are the state machine for selecting the visual servoing control law and the Bayesian inference used to handle ambiguities in the feature estimations.

The visual servoing control loop is shown in Figure 4.6. Each iteration of the control loop starts by segmenting the needle from the US image. The segmentation uses two image filters and segments the filtered images individually. Then these two segmentations are combined in order to produce a final segmentation of the needle.

The visual features are extracted from the segmented image mainly using image moments. There are two models of the needle, one where the needle is intersecting the image plane and one where the needle is aligned with the needle plane. Which model is used and which features are extracted depends on the state of the state machine. The visual features are filtered using a Kalman filter, and in some cases the Kalman filter estimates some features, as these cannot be extracted from the image. One issue with some of the visual features is that their sign is ambiguous. A probabilistic method for determining the sign using Bayesian theory is presented in the paper.

The US probe is controlled using classical image-based visual servoing [18] with visual features depending on the state machine. The state machine keeps track of the relative pose between the needle and the US probe, as different control schemes are required for different poses.

Both simulation and experiments were conducted to verify the correctness of the proposed method. In the simulation a simplified synthetic US image is created. The simulation is used to verify that the method functions as intended, but does not check the robustness of the method. In the experiment a biopsy needle was submerged in a water tank, shown in Figure 4.7. The robot positions the US probe so that the image plane intersects the needle before the experiment starts, and then the proposed method is started.

The simulation showed a very stable approach to minimizing visual feature errors, and even-

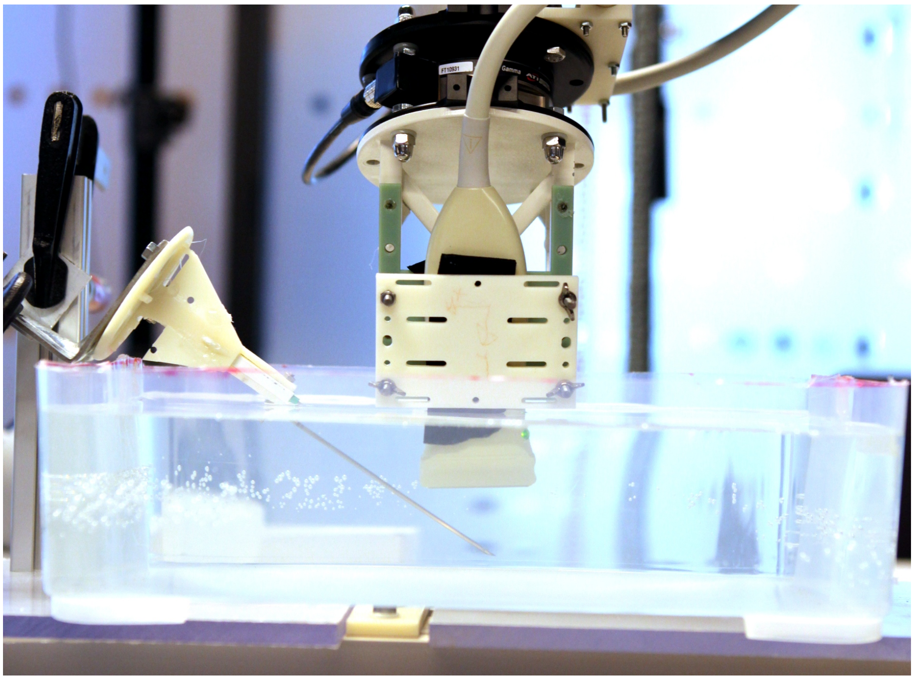

Figure 4.7: The experiment setup in Paper IV, consisting of a UR5 robot (Universal Robots) moving the ultrasound probe, a water tank and a biopsy needle.

tually to aligning the needle and image plane. In the robot experiment the approach was less stable, but still managed to align the probe. In both the simulation and the robot experiment it took between 45 s and 60 s to align the probe, which is too long for any practical use of the method. The control gains could not be increased further, because of a delay in acquiring the images. This delay caused unstable control for higher gains. However, simulations indicated that the gains could be increased if the delay were decreased.

Chapter 5

Discussion

This section discusses the work presented in the thesis. First, the approach and design choices are treated in Section 5.1, followed by a discussion of the results in Section 5.2. In Section 5.3 limitations of the research in this thesis are presented. Finally, in Section 5.4, possible impacts of the research are indicated.

5.1 Approaches and design choices

In addressing the aims of the thesis, a number of design choices were made. First of all, the thesis assumes that two individual robotic arms are manipulating the needle and US probe. A different approach would be to have the US probe and needle insertion device mounted on the same robot, as done in [32]. This latter method has some clear benefits. First of all, the needle is rigidly attached to the probe, which means that it is less likely that the needle will go out of the image plane during insertion. Other benefits are that less registration is required, and that the needle path is more fixed and known when inserting the needle. A disadvantage of using only one arm is that this limits the movement possibilities of the ultrasound probe. When the needle has penetrated the skin, moving the probe would also move the needle which is inside the body. This could hurt or injure the patient and even break the needle. Therefore, only small adjustments can be made, or the probe needs to move independently of the needle.

The advantage of using two robots is that the system is more flexible as a general system for medical intervention. First of all, robotic ultrasound systems may be used in other contexts. As already seen in Chapter 2, there are a wide variety of applications for such systems, and a stand-alone system can be more easily adapted to other applications. The needle insertion robot may also have other areas of application. This was the case in [59] where a robot that was developed for needle insertion was later used for cutting and suturing; the robotic ultrasound system was a stand alone system.

Although this thesis envisions a two-robot approach, it does not mean that the developed methods cannot be used in a one-robot setup. First of all, the platform developed in Paper I can be expanded by adding a needle insertion device to the robot tool. Second, the needle tracking methods developed in Papers II and III include no assumptions about whether one or two robots are used, thus no changes to these components are required. The visual servoing in Paper IV might not be needed, or would have to be altered for a one-robot setup. Because the needle is rigidly attached to the probe there is less need for adjustments. On the other hand, this imposes movement restrictions, which the method in Paper IV does not take into account. Therefore, the method must be modified for a one-robot approach.

In this thesis we have used a commercially available, collaborative[1] robot. This differs from the majority of previous research in the field, which mostly uses custom robots. One clear benefit of using a commercial robot is that the time used to commercialize and apply the research in the clinic is much less, as the robot is already in production. Another benefit is that the robot is already certified as a collaborative robot, which means that no safety guards are required and the robot can operate directly with humans. Although no ISO standard yet exists for surgical robots, ISO is working on one, which will make the certification process easier. A benefit of creating a custom robot is that it is designed for a specific task, and thus will probably function better at performing that task.

An in-plane needle insertion approach is considered in this thesis. The benefit of this approach is that the whole needle is visible along with the target. In addition, is possible to see if there are any critical regions that should be avoided in the needle path. This approach has received the most attention from researchers. Its disadvantage is the possibility that slight deviations from the image plane by the needle, either from needle bending or erroneous insertion, will cause poor needle visibility in the image or that parts of the needle are not imaged. The other approach, out-of-plane insertion, has reverse advantages and disadvantages as the in-plane approach. This approach involves moving the probe back and forth to always ensure that the needle tip is visible as it advances. Needle bending is not an issue because the cross-section of the needle is imaged. The disadvantage of this approach is that it is not possible to view the target and needle at the same time or to see any critical regions in the needle path as it advances. In [85] a visual servoing method is presented that follows the needle tip as it is inserted out-of-plane, and is an example of work dealing with out-of-plane needle estimation. Our view is that the benefits of the in-plane approach are much greater than the disadvantages, especially as Paper IV proposes a possible solution to the problem of the needle not being aligned with the image plane.

5.2 Performance

5.2.1 Robotic ultrasound system

A set of requirements based on state-of-the-art systems is derived in Paper I. These requirements represent a scientific contribution because they are more complete than previously published requirements. The developed ultrasound robotic system meets the requirements, with some small exceptions. The video frame rate is lower than the requirement, at 23.9 frames/s compared to the required 25 frames/s. There is also a delay of approximately 200 ms from when the images are acquired in the US machine until they arrive in the control computer. Both these effects are the result of using a frame grabber rather than accessing the images directly on the US machine. An advantage of using the frame grabber is that any US machine may be used. The disadvantage is that the frame rate becomes more unstable and a delay is introduced.

[1]According to EN ISO 10218-1:2006

Three different control schemes have been implemented in the system: force and haptic control in Paper I and visual servoing in Paper IV. The force control scheme is estimated to have a bandwidth of 16.6 Hz, which is much higher than the required 3 Hz. The main purpose of the force control is to maintain contact with the tissue. One of the main disturbances will be respiratory motion of the patient. Movement of the chest during respiration is relatively small and below 5 mm during tidal breathing [24]. By analyzing the chest movement given in [24] we have estimated that the bandwidth of the respiration is below 1.5 Hz, with its main component at approximately 0.3 Hz. The force controller will be able to compensate for the respiratory motion.

Transparency is often used as a performance measure for haptic control. In [89] transparency is defined as master impedance divided by slave impedance, and *good transparency* is defined to be where the magnitude of the transparency is between ± 3 dB and the phase is between $\pm 45°$. The transparency bandwidth of the controller is 39.5 Hz and the controller has good transparency up to 1.2 Hz. [89] reports that their system achieved good transparency up to 0.5 Hz, 1 Hz and 6 Hz when in contact with fat, muscle and the ribcage respectively. The system reported here has good transparency up to 1.2 Hz when in contact with a soft medium. This is comparable with the results in [89]. The position control loop is the main impediment to achieving good transparency at higher frequencies. Using a more sophisticated controller rather than the proportional controller might yield good transparency for higher frequencies.

The visual servoing method presented in Paper IV is assessed qualitatively, as only one experiment is reported in the paper. It is not possible to directly compare the results to other visual servoing methods, as no other method exists to align a 2D ultrasound probe plane with a needle. In [17] a 3D probe is controlled using a visual servoing scheme, but this a quite different problem. When using visual servoing with a 3D probe, the needle tracking problem is solved first and then the probe is controlled based on the estimated needle position. In our application it is the other way around, as the needle first needs to be in the imaging plane before the tracking can start.

5.2.2 Needle tracking

There are two main performance metrics to consider in the needle tracking methods. First is that they should have high accuracy and precision, and this is the first priority. The second metric is that they should be executed in real-time. The accuracy and precision of the methods will be discussed first, then the real-time properties of the methods.

Two sets of experiments have been conducted to quantify the tracking error. In Paper II, only the errors of the method presented in the paper were quantified while in Paper III, the method in Paper II, the method in [25] (denoted DF) and the novel methods of Paper III were all used on the same dataset.

There are two main error metrics to consider in needle tracking methods: the error in estimated insertion angle and the error in estimated tip position (which is a 2D vector). It is useful to decompose this vector into an error that uses the needle axis as its basis vector and an error that is perpendicular to the needle axis. This separates two different processes in the estimation, namely estimating the axis and estimating the tip position.

Comparing the results of the method in Paper II (denoted OM) with the experiments in

Papers II and III, it is apparent that it is more difficult to estimate the needle in the dataset in Paper III. The OM method had larger errors in both the insertion angle and position along the needle, but the error perpendicular to the needle was comparable. Also, the DF method performed much more poorly than in the original paper.

For the methods presented in Paper III, the reduction of the standard deviation of the error for the position along the needle is significant for both KF+F and KF_v+F when comparing with OM, and KF_v+F has significantly lower values than KF+F. There was also a substantial reduction in the 95th percentile of the error, and the standard deviation of the insertion angle error was reduced significantly.

One of the main differences between the methods in Paper II and III is the introduction of statistical filters (Kalman filter and particle filter). The OM method had a problem with some samples being far from the correct value. These outliers are effectively filtered using a Kalman filter.

It is worth noting that the KF+F method does not require the measurement of insertion velocity and can therefore also be used when a physician manually inserts a needle.

For the methods to be classified as real-time methods, they need to finish processing one US image before the next one is available for processing. In Paper II the maximum execution time for one US image was 19.2 ms, while in Paper III it increased to 28.2 ms. The increase is due to some changes in the image filters. Because a different US machine was used, the filters needed to be adapted to the resolution and image size provided by the new machine. Moreover, the OM method increased its maximum execution time to 27.4 ms. The introduction of statistical filters did not affect the execution time notably, as many of the methods using a statistical filter had lower maximum execution time than the OM method. The methods used in Paper III can run in real-time at a frame rate of 34 frames per second.

5.3 Limitations

Paper I showed that it is feasible to use a collaborative industrial robot to create a robotic ultrasound system, but there are some shortcomings. First of all, the haptic control is only tested when the master and slave robot are in the same room. Technically, it should be easy to separate the master and slave and to communicate over IP because the control systems are implemented as two processes communicating through a real-time pipe. However, it is hard to know how the performance will be when there is a time delay in the transmission of data between the two devices. The system remains to be tested by physicians, which could give many valuable insights on how to improve the system and streamline it for clinical use.

The method presented in Paper II estimated the needle tip position far from the correct location for some images. This happens when the combined feature function $h(x)$ has its maximum far from the needle tip location. This typically happens when the functions has two or more peaks and the peak value at the needle tip location is lower than the peak value at another location. These outliers could make it hard to use the method in a real application using a robot to insert the needle.

The method presented in Paper III removes most of the outliers compared to the method in Paper II and is therefore more robust in its estimation. Both the needle estimation methods assumes a rigid needle. The methods use an improved version of the axis estimation in [68] where bending needles are detected. With a few modifications, our method could also work on bending needles. The main modifications would be to calculate the features along the curved needle instead of along a straight line when estimating the needle tip location. This would require some interpolation of image pixels, but would theoretically be the same as the current method. The reason for using a relatively large diameter needle and assuming that it is rigid is that quantitative errors are more easily obtained.

One drawback with the needle tracking methods presented in this thesis is that the needle must lie in the image plane. This can be hard to achieve using a robot, even with accurate tracking and registration. The visual servoing method presented in Paper IV addresses this issue, but these two methods have not been tested together, and therefore it is unknown how the visual servoing control will affect the estimation. It is likely that some kind of communication between the methods is required, for instance that the visual servoing method informs the tracking method that the needle is aligned and possibly gives some indication of image quality. The image quality metric could be the distance between the needle center and the image plane, which is one of the features in the visual servoing method.

Another control method that could influence the tracking performance is the force control. It would control the probe in the y-direction of the US image. It should, however, be fairly simple to compensate for the probe movement, as it is measured by the robot. However, the method would need to be updated in order to incorporate this new information.

The proposed method in Paper IV has some possible areas of improvement. First of all, there are some instances where the US probe is controlled solely based on estimated visual features. This could be problematic as the visual information in the image is not used, resulting in an open control loop. Another issue is the segmentation of the needle. In the paper it is rather easy to segment the needle because a water tank was used in the experiment, which made the images very clear and the needle stand out. In reality, it is a quite hard problem, as the images of tissue are noisy and have many structures that could interfere with segmentation. The simulations in the paper do not use realistic US images, because their purpose is to validate that the method functions correctly. It would have been beneficial to do a realistic simulation to test the robustness of the proposed method in a controlled manner.

The methods from the different papers in this thesis have not been tested together. For a complete needle tracking sensing system, the US probe should be controlled using a hybrid approach, as already mentioned. One degree of freedom should be force controlled to ensure physical contact with the tissue, and the other five degrees of freedom should be controlled using a visual servoing approach to ensure that the needle is visible in the image. The two control methods could influence each other (and the tracking method) in unknown ways, and the methods might need some modifications to handle the influence from the other methods.

5.4 Impact

Previous research within robotic ultrasound has led to one commercial product, Estele from Robosoft, France. This robot is a hand-held system intended for emergency care or to be used on a space station, and was developed in cooperation with the University of Bourges, France.

In Norway there is a government reform to shift more health care responsibility to the local health care centers (Samhandlingsreformen), and with the increasing availability of ultrasound machines at local health care centers a new market could emerge for tele-operated ultrasound machines. Because the results of ultrasound examinations depend on skill it would be beneficial if local physicians could get help from a regional health service through tele-operation whenever a second opinion is needed. With a teleoperated system the patient could be examined the same day, rather than having to wait for a new appointment and travel to a regional health care center.

Paper I found that it is feasible to create such a tele-operated system using a commercial robot. As a result, the software has been licensed to Mektron AS, which plans to commercialize the platform.

One possible medical impact of this research is the use of the needle tracking methods from Papers II and III to aid physicians when inserting needles. The methods from Paper II include no assumptions about a robot inserting the needle, and the methods in Paper III are validated both with and without measurements from the robot. This will, however, require some further research in order to verify that such a visual aid will have a positive effect on medical outcomes.

If an autonomous needle insertion system is realized it could have several positive medical outcomes. In biopsy procedures, higher accuracy should result in fewer biopsy needle insertions missing the target. There are two possible outcomes if the target is missed. First, is if it is detected by the physician, he or she will have to redo the biopsy, making another insertion and causing discomfort to the patient and using more time to complete the procedure. A robotic system with higher accuracy would then decrease patient discomfort and execution time. Second, is if it is not detected that the biopsy missed its target it could lead to a malignant tumor not being detected. In such cases, higher accuracy might lead to more accurate diagnostics.

For ablation procedures, higher insertion accuracy could lead to better tumor coverage. The ablation probe should be inserted such that the tumor is covered by a certain margin, and at the same time ablate as little healthy tissue as possible. Higher accuracy in the insertion will place the probe closer to the target, and as a result there is a higher chance that the whole tumor is covered.

Chapter 6

Conclusion

This thesis has contributed in making an active sensing system for autonomous needle insertion by a robot. The thesis describes a robotic system for monitoring the insertion of a needle and a method for estimating the needle axis and tip using ultrasound images and robot velocity. The components have been tested individually. The main contributions of this thesis can be summarized as follows:

- It has been showed that it is feasible to use the UR5 robot from Universal Robots to create an ultrasound robotic system. The main innovation is the use of a collaborative, commercially available industry robot, which has not been done before. This enables fast transfer from research to commercial product, which is further supported by the licensing of the software to Mektron AS.

- The ultrasound robotic system in this thesis implements both force and haptic control, both of which are shown to have bandwidth comparable to other systems and to meet the required bandwidth.

- A novel needle tracking method is demonstrated. It incorporates a dynamic region of interest, defined by the estimated needle tip position from the previous time step. It detects the needle tip using a linear combination of five features and uses statistical filtering to make the method more robust against outliers. The method estimates the needle accurately and improves precision significantly compared to other methods.

- The needle tracking method is able to track the needle in real time, and it is shown that using velocity measured by the robot inserting the needle significantly increases both the accuracy and the precision of the estimation.

- A novel visual servoing method is shown to align the imaging plane of a 2D ultrasound probe with a biopsy needle. The method shows promise for solving the alignment problem.

6.1 Future work

Future work will include verifying that the individual components can be integrated together. The force control of the US probe must be integrated with the visual servoing of the probe.

As already mentioned, this should not pose much difficulty as the two controllers will control separate directions in tool space. Another issue is how the needle tracking is affected by the visual servoing. This is an open issue and needs experimental validation. Some adjustments will probably be needed both in the visual servoing method and the tracking method for them to work together. The tracking method must incorporate the movement of the probe, and the visual servoing method might need to signal the tracking algorithm when the needle is aligned in the image plane.

Before all the components can be integrated, the visual servoing method needs to be adjusted to work with real tissue. The segmentation of the needle is simplified in this thesis, as only a water tank is considered. The segmentation method must be improved to be able to segment the needle from tissue in the US images.

The teleoperation of the developed robotic system was only tested in a local setting, and not by physicians. A study where physicians use the teleoperated robot is needed. This will validate whether it is feasible for the physician to use the system in a clinical setting. Another line of research would be to use the developed system in a remote setting for telediagnostics, where the physician and patient are located at different sites. A study of the usability of the system with transmission delay and video conferencing between the physician and patient is needed to check if the system performs adequately under these conditions or if further improvements are needed.

Bibliography

[1] MIL-STD-1629 A Procedures for performing a failure mode, effects and criticality analysis. Technical report, Department of Defence, United States of America, November 1980.

[2] *Concise Medical Dictionary*. Oxford University Press (OUP), jan 2010. doi:10.1093/acref/9780199557141.001.0001.

[3] Estele - robotic system for tele-echography, January 2012. Available from: www.robosoft.fr.

[4] Niki Abolhassani, Rajni Patel, and Mehrdad Moallem. Needle insertion into soft tissue: A survey. *Medical Engineering & Physics*, 29(4):413–431, may 2007. doi:10.1016/j.medengphy.2006.07.003.

[5] P. Abolmaesumi, S.E. Salcudean, Wen-Hong Zhu, M.R. Sirouspour, and S.P. DiMaio. Image-guided control of a robot for medical ultrasound. *IEEE Trans. Robot. Automat.*, 18(1):11–23, 2002. doi:10.1109/70.988970.

[6] Fikri M Abu-Zidan, Ashraf F Hefny, and Peter Corr. Clinical ultrasound physics. *Journal of Emergencies, Trauma and Shock*, 4(4):501, 2011. doi:10.4103/0974-2700.86646.

[7] Muneeb Ahmed, Christopher L Brace, Fred T Lee, and S Nahum Goldberg. Principles of and advances in percutaneous ablation. *Radiology*, 258(2):351–369, 2011. doi:10.1148/radiol.10081634.

[8] Kamran Ahrar and Sanjay Gupta, editors. *Percutaneous Image-Guided Biopsy*. Springer Science & Business Media, 2014. doi:10.1007/978-1-4614-8217-8.

[9] Ph. Arbeille, J. Ayoub, V. Kieffer, P. Ruiz, B. Combes, A. Coitrieux, P. Herve, S. Garnier, B. Leportz, E. Lefbvre, and F. Perrotin. Realtime tele-operated abdominal and fetal echography in 4 medical centres, from one expert center, using a robotic arm & ISDN or satellite link. In *2008 IEEE International Conference on Automation, Quality and Testing, Robotics*, volume 1, pages 45–46. Institute of Electrical & Electronics Engineers (IEEE), 2008. doi:10.1109/aqtr.2008.4588703.

[10] A. Ayvaci, P. Yan, S. Xu, S. Soatto, and J. Kruecker. Biopsy needle detection in transrectal ultrasound. *Computerized Medical Imaging and Graphics*, 2011.

[11] W. Bachta and A. Krupa. Towards ultrasound image-based visual servoing. In *Proceedings 2006 IEEE International Conference on Robotics and Automation, 2006. ICRA 2006.*,

pages 4112–4117. Institute of Electrical & Electronics Engineers (IEEE), 2006. doi:10.1109/robot.2006.1642334.

[12] M. Barva, J. Kybic, J.M. Mari, C. Cachard, and V. Hlavác. Automatic localization of curvilinear object in 3d ultrasound images. *Biomedical Engineering, Czech Technical University, Czech Republic, SPIE*, 10, 2005.

[13] E.M. Boctor, M.A. Choti, E.C. Burdette, and R.J. Webster Iii. Three-dimensional ultrasound-guided robotic needle placement: an experimental evaluation. *The International Journal of Medical Robotics and Computer Assisted Surgery*, 4(2):180–191, 2008. doi:10.1002/rcs.184.

[14] M. Bonfe, F. Boriero, R. Dodi, P. Fiorini, A. Morandi, R. Muradore, L. Pasquale, A. Sanna, and C. Secchi. Towards automated surgical robotics: A requirements engineering approach. In *Biomedical Robotics and Biomechatronics (BioRob), 2012 4th IEEE RAS & EMBS International Conference on*, pages 56–61. IEEE, 2012. doi:10.1109/biorob.2012.6290700.

[15] F. Bruyère, J. Ayoub, and P. Arbeille. Use of a Telerobotic Arm to Perform Ultrasound Guidance During Renal Biopsy in Transplant Recipients: A Preliminary Study. *Journal of Endourology*, pages 317–322, 2010. doi:10.1089/end.2010.0287.

[16] G. Charron, N. Morette, T. Essomba, P. Vieyres, J. Canou, P. Fraisse, S. Zeghloul, A. Krupa, P.Arbeille, and The PROSIT consortium. Robotic platform for an interactive tele-echographic system: The prosit anr-2008 project. In *Hamlyn Symposium on medical robotics*, pages 1–2, 2010.

[17] Pierre Chatelain, Alexandre Krupa, and Maud Marchal. Real-time needle detection and tracking using a visually servoed 3d ultrasound probe. In *2013 IEEE International Conference on Robotics and Automation*, pages 1668–1673. Institute of Electrical & Electronics Engineers (IEEE), may 2013. doi:10.1109/icra.2013.6630795.

[18] F. Chaumette and S. Hutchinson. Visual servo control, part i: Basic approaches. *IEEE Robotics and Automation Magazine*, 13(4):82–90, 2006.

[19] K. Chin, A. Perlas, V. Chan, and R. Brull. Needle visualization in ultrasound-guided regional anesthesia: Challenges and solutions. *Regional Anesthesia and Pain Medicine*, 33(6):532–544, nov 2008. doi:10.1016/j.rapm.2008.06.002.

[20] D.W. Cool, L. Gardi, C. Romagnoli, M. Saikaly, J.I. Izawa, and A. Fenster. Temporal-based needle segmentation algorithm for transrectal ultrasound prostate biopsy procedures. *Medical physics*, 37:1660, 2010.

[21] F. Courreges, P. Vieyres, and RS Istepanian. Advances in robotic tele-echography services–the OTELO system. In *Conference proceedings: Annual International Conference of the IEEE Engineering in Medicine and Biology Society. IEEE Engineering in Medicine and Biology Society. Conference*, volume 7, page 5371, 2004. doi:10.1109/iembs.2004.1404499.

[22] B. Davies. Safety of medical robots. *Safety-Critical Systems: Current Issues, Techniques and Standards*, pages 193–201, 1993.

[23] D. De Cunha, P. Gravez, C. Leroy, E. Maillard, J. Jouan, P. Varley, M. Jones, M. Halliwell, D. Hawkes, PNT Wells, et al. The midstep system for ultrasound guided remote telesurgery. In *Engineering in Medicine and Biology Society, 1998. Proceedings of the 20th Annual International Conference of the IEEE*, volume 3, pages 1266–1269. IEEE, 1998. doi:10.1109/iembs.1998.747107.

[24] Anne De Groote, Muriel Wantier, Guy Chéron, Marc Estenne, and Manuel Paiva. Chest wall motion during tidal breathing. *Journal of Applied Physiology*, 83(5):1531–1537, 1997.

[25] M. Ding and A. Fenster. A real-time biopsy needle segmentation technique using hough transform. *Medical physics*, 30:2222, 2003.

[26] G. Dogangil, BL Davies, and F. Rodriguez y Baena. A review of medical robotics for minimally invasive soft tissue surgery. *Proceedings of the Institution of Mechanical Engineers, Part H: Journal of Engineering in Medicine*, 224(5):653–679, 2010. doi:10.1243/09544119jeim591.

[27] Katharine J. Draper, Christopher C. Blake, Linda Gowman, Donal B. Downey, and Aaron Fenster. An algorithm for automatic needle localization in ultrasound-guided breast biopsies. *Med. Phys.*, 27(8):1971, 2000. doi:10.1118/1.1287437.

[28] S. Nahum Goldberg, G. Scott Gazelle, and Peter R. Mueller. Thermal ablation therapy for focal malignancy. *American Journal of Roentgenology*, 174(2):323–331, feb 2000. doi:10.2214/ajr.174.2.1740323.

[29] S. Nahum Goldberg, Clement J. Grassi, John F. Cardella, J. William Charboneau, Gerald D. Dodd, Damian E. Dupuy, Debra Gervais, Alice R. Gillams, Robert A. Kane, Fred T. Lee, Tito Livraghi, John McGahan, David A. Phillips, Hyunchul Rhim, and Stuart G. Silverman. Image-guided tumor ablation: Standardization of terminology and reporting criteria1. *Radiology*, 235(3):728–739, jun 2005. doi:10.1148/radiol.2353042205.

[30] A. Gourdon, P. Poignet, G. Poisson, P. Vieyres, and P. Marche. A new robotic mechanism for medical application. In *Advanced Intelligent Mechatronics, 1999. Proceedings. 1999 IEEE/ASME International Conference on*, pages 33–38. IEEE, 1999. doi:10.1109/aim.1999.803139.

[31] M Halliwell. A tutorial on ultrasonic physics and imaging techniques. *Proceedings of the Institution of Mechanical Engineers, Part H: Journal of Engineering in Medicine*, 224(2):127–142, 2010. doi:10.1243/09544119JEIM656.

[32] J Hong, T Dohi, M Hashizume, K Konishi, and N Hata. An ultrasound-driven needle-insertion robot for percutaneous cholecystostomy. *Physics in Medicine and Biology*, 49(3):441–455, jan 2004. doi:10.1088/0031-9155/49/3/007.

[33] Jae-Sung Hong, Takeyoshi Dohi, Makoto Hasizume, Kozo Konishi, and Nobuhiko Hata. A motion adaptable needle placement instrument based on tumor specific ultrasonic image segmentation. In *Medical Image Computing and Computer-Assisted Intervention — MICCAI 2002*, pages 122–129. Springer Science + Business Media, 2002. doi: 10.1007/3-540-45786-0_16.

[34] Marie-Ange Janvier, Louis-Gilles Durand, Marie-Hélène Roy Cardinal, Isabelle Renaud, Boris Chayer, Pascal Bigras, Jacques de Guise, Gilles Soulez, and Guy Cloutier. Performance evaluation of a medical robotic 3d-ultrasound imaging system. *Medical image analysis*, 12(3):275–290, 2008. doi:10.1016/j.media.2007.10.006.

[35] Marie-Ange Janvier, Gilles Soulez, Louise Allard, and Guy Cloutier. Validation of 3d reconstructions of a mimicked femoral artery with an ultrasound imaging robotic system. *Medical physics*, 37(7):3868–3879, 2010. doi:10.1118/1.3447721.

[36] M. P. Kadaba, P. K. Bhagat, and V. C. Wu. Attenuation and backscattering of ultrasound in freshly excised animal tissues. *IEEE Transactions on Biomedical Engineering*, BME-27(2):76–83, Feb 1980. doi:10.1109/TBME.1980.326710.

[37] M. Kaya and O. Bebek. Gabor filter based localization of needles in ultrasound guided robotic interventions. In *Imaging Systems and Techniques (IST), 2014 IEEE International Conference on*, pages 112–117, Oct 2014. doi:10.1109/IST.2014.6958456.

[38] M. Kaya and O. Bebek. Needle localization using gabor filtering in 2d ultrasound images. In *Robotics and Automation (ICRA), 2014 IEEE International Conference on*, pages 4881–4886, May 2014. doi:10.1109/ICRA.2014.6907574.

[39] Mert Kaya, Enes Senel, Awais Ahmad, Orcun Orhan, and Ozkan Bebek. Real-time needle tip localization in 2d ultrasound images for robotic biopsies. In *2015 International Conference on Advanced Robotics (ICAR)*. Institute of Electrical & Electronics Engineers (IEEE), jul 2015. doi:10.1109/icar.2015.7251432.

[40] Riccardo Muradore Paolo Fiorini Kim Mathiassen, Diego Dall'Alba and Ole Jakob Elle. Robust real-time needle tracking in 2d ultrasound images using statistical filtering. *IEEE Transactions on Control System Technology*. doi:10.1109/TCST.2016.2587733.

[41] N. Koizumi, S. Warisawa, H. Hashizume, and M. Mitsuishi. Dynamic Switching of a Controller Based on Diagnostic Tasks in Remote Ultrasound Diagnostics. *Journal of Robotics and Mechatronics*, 16(2):146–154, 2004.

[42] H.I. Krebs, J.J. Palazzolo, L. Dipietro, M. Ferraro, J. Krol, K. Rannekleiv, B.T. Volpe, and N. Hogan. Rehabilitation robotics: Performance-based progressive robot-assisted therapy. *Autonomous Robots*, 15(1):7–20, 2003. doi:10.1023/A:1024494031121.

[43] A. Krupa, G. Fichtinger, and G. D. Hager. Real-time motion stabilization with b-mode ultrasound using image speckle information and visual servoing. *The International Journal of Robotics Research*, 28(10):1334–1354, 2009. doi:10.1177/0278364909104066.

[44] Alexandre Krupa, Gabor Fichtinger, and Gregory D. Hager. Full motion tracking in ultrasound using image speckle information and visual servoing. In *Proceedings 2007 IEEE International Conference on Robotics and Automation*, pages 2458–2464. Institute of Electrical & Electronics Engineers (IEEE), apr 2007. doi:10.1109/robot.2007.363688.

[45] Deukhee Lee, Norihiro Koizumi, Kohei Ota, Shin Yoshizawa, Akira Ito, Yukio Kaneko, Yoichiro Matsumoto, and Mamoru Mitsuishi. Ultrasound-based visual servoing system for lithotripsy. In *2007 IEEE/RSJ International Conference on Intelligent Robots and Systems*, pages 877–882. Institute of Electrical & Electronics Engineers (IEEE), oct 2007. doi:10.1109/iros.2007.4399363.

[46] V.G. Mallapragada, N. Sarkar, and T.K. Podder. Robot assisted real-time tumor manipulation for breast biopsy. pages 2515–2520, May 2008. doi:10.1109/ROBOT.2008.4543591.

[47] Vishnu Mallapragada, Nilanjan Sarkar, and Tarun K. Podder. Toward a robot-assisted breast intervention system. *IEEE/ASME Transactions on Mechatronics*, 16(6):1011–1020, dec 2011. doi:10.1109/tmech.2010.2068575.

[48] Vishnu G. Mallapragada, Nilanjan Sarkar, and Tarun K. Podder. Autonomous coordination of imaging and tumor manipulation for robot assisted breast biopsy. In *2008 2nd IEEE RAS & EMBS International Conference on Biomedical Robotics and Biomechatronics*, pages 676–681. Institute of Electrical & Electronics Engineers (IEEE), oct 2008. doi: 10.1109/biorob.2008.4762815.

[49] Thomas Martinelli, Jean-Luc Bosson, Luc Bressollette, Franck Pelissier, Eric Boidard, Jocelyne Troccaz, and Philippe Cinquin. Robot-based tele-echography - Clinical evaluation of the TER system in abdominal aortic exploration. *JOURNAL OF ULTRASOUND IN MEDICINE*, 26(11):1611–1616, 2007.

[50] K. Masuda, E. Kimura, N. Tateishi, and K. Ishihara. Three dimensional motion mechanism of ultrasound probe and its application for tele-echography system. In *Intelligent Robots and Systems, 2001. Proceedings. 2001 IEEE/RSJ International Conference on*, volume 2, pages 1112–1116. IEEE, 2001. doi:10.1109/iros.2001.976317.

[51] Kohji Masuda, Yuuki Takachi, Yasuhiro Urayama, and Takashi Yoshinaga. Development of support system to handle ultrasound probe by coordinated motion with medical robot. In *Engineering in Medicine and Biology Society, EMBC, 2011 Annual International Conference of the IEEE*, pages 4519–4522. IEEE, 2011. doi:10.1109/iembs.2011.6091120.

[52] Kim Mathiassen, Diego Dall'Alba, Riccardo Muradore, Paolo Fiorini, and Ole Jakob Elle. Real-time biopsy needle tip estimation in 2d ultrasound images. In *Robotics and Automation (ICRA), 2013 IEEE International Conference on*, pages 4363–4369, May 2013. doi:10.1109/ICRA.2013.6631195.

[53] Kim Mathiassen, Jørgen Enger Fjellin, Kyrre Glette, Per Kristian Hol, and Ole Jakob Elle. An ultrasound robotic system using the commercial robot ur5. *Frontiers in Robotics and AI*, 3(1), 2016. doi:10.3389/frobt.2016.00001.

[54] Kim Mathiassen, Kyrre Glette, and Ole Jakob Elle. Visual servoing of a medical ultrasound probe for needle insertion. In *2016 IEEE International Conference on Robotics and Automation (ICRA)*, pages 3426–3433, May 2016. doi:10.1109/ICRA.2016.7487520.

[55] R. Mebarki, A. Krupa, and F. Chaumette. 2-d ultrasound probe complete guidance by visual servoing using image moments. *IEEE Trans. Robot.*, 26(2):296–306, apr 2010. doi:10.1109/tro.2010.2042533.

[56] Rafik Mebarki, Alexandre Krupa, and Francois Chaumette. Image moments-based ultrasound visual servoing. In *2008 IEEE International Conference on Robotics and Automation*, pages 113–119. Institute of Electrical & Electronics Engineers (IEEE), may 2008. doi:10.1109/robot.2008.4543195.

[57] Rafik Mebarki, Alexandre Krupa, and Francois Chaumette. Modeling and 3d local estimation for in-plane and out-of-plane motion guidance by 2d ultrasound-based visual servoing. In *2009 IEEE International Conference on Robotics and Automation*. Institute of Electrical & Electronics Engineers (IEEE), may 2009. doi:10.1109/robot.2009.5152371.

[58] M. Mitsuishi, S. Warisawa, T. Tsuda, T. Higuchi, N. Koizumi, H. Hashizume, and K. Fujiwara. Remote ultrasound diagnostic system. In *IEEE International Conference on Robotics and Automation, 2001. Proceedings 2001 ICRA*, pages 1567–1574, 2001. doi:10.1109/robot.2001.932834.

[59] Riccardo Muradore, Paolo Fiorini, Gokhan Akgun, Duygun Erol Barkana, Marcello Bonfe, Fabrizio Boriero, Andrea Caprara, Giacomo De Rossi, Riccardo Dodi, Ole Jakob Elle, Federica Ferraguti, Lorenza Gasperotti, Roger Gassert, Kim Mathiassen, Dilla Handini, Olivier Lambercy, Lin Li, Maarja Kruusmaa, Auralius Oberman Manurung, Giovanni Meruzzi, Ho Quoc Phuong Nguyen, Nicola Preda, Gianluca Riolfo, Asko Ristolainen, Alberto Sanna, Cristian Secchi, Marco Torsello, and Asım Evren Yantac. Development of a cognitive robotic system for simple surgical tasks. *International Journal of Advanced Robotic Systems*, 12, 2015. doi:10.5772/60137.

[60] C Nadeau and A Krupa. A multi-plane approach for ultrasound visual servoing: Application to a registration task. In *2010 IEEE/RSJ International Conference on Intelligent Robots and Systems*, pages 5706–5711. Institute of Electrical & Electronics Engineers (IEEE), oct 2010. doi:10.1109/iros.2010.5651463.

[61] Caroline Nadeau and Alexandre Krupa. Intensity-based direct visual servoing of an ultrasound probe. In *2011 IEEE International Conference on Robotics and Automation*, pages 5677–5682. Institute of Electrical & Electronics Engineers (IEEE), may 2011. doi:10.1109/icra.2011.5979673.

[62] E. Naerum and B. Hannaford. Global transparency analysis of the lawrence teleoperator architecture. In *2009 IEEE International Conference on Robotics and Automation*. Institute of Electrical & Electronics Engineers (IEEE), may 2009. doi:10.1109/robot.2009.5152791.

[63] Ryu Nakadate, Jorge Solis, Atsuo Takanishi, Motoaki Sugawara, Kiyomi Niki, and Eiichi Minagawa. Development of the ultrasound probe holding robot wta-1rii and an automated scanning algorithm based on ultrasound image feedback. In *ROMANSY 18 Robot Design, Dynamics and Control*, volume 524, pages 359–366. Springer Vienna, 2010. doi:10.1007/978-3-7091-0277-0_42.

[64] Ryu Nakadate, Yasuaki Tokunaga, Jorge Solis, Atsuo Takanishi, Eiichi Minagawa, Motoaki Sugawara, Kiyomi Niki, and Akiko Saito. Development of robot assisted measurement system for abdominal ultrasound diagnosis. In *Biomedical Robotics and Biomechatronics (BioRob), 2010 3rd IEEE RAS and EMBS International Conference on*, pages 367–372. IEEE, 2010. doi:10.1109/biorob.2010.5627716.

[65] H.R.S. Neshat and R.V. Patel. Real-time parametric curved needle segmentation in 3d ultrasound images. In *Biomedical Robotics and Biomechatronics, 2008. BioRob 2008. 2nd IEEE RAS & EMBS International Conference on*, pages 670–675. Ieee, 2008.

[66] Alexander Ng and Justiaan Swanevelder. Resolution in ultrasound imaging. *Continuing Education in Anaesthesia, Critical Care & Pain*, 11(5):186–192, 2011. doi:10.1093/bjaceaccp/mkr030.

[67] P.M. Novotny, J.A. Stoll, N.V. Vasilyev, P.J. Del Nido, P.E. Dupont, T.E. Zickler, and R.D. Howe. Gpu based real-time instrument tracking with three-dimensional ultrasound. *Medical image analysis*, 11(5):458–464, 2007.

[68] S.H. Okazawa, R. Ebrahimi, J. Chuang, R.N. Rohling, and S.E. Salcudean. Methods for segmenting curved needles in ultrasound images. *Medical image analysis*, 10(3):330–342, 2006.

[69] Terry Peters and Kevin Cleary, editors. *Image-Guided Interventions*. Springer Science + Business Media, 2008. doi:10.1007/978-0-387-73858-1.

[70] F. Pierrot, E. Dombre, E. Dégoulange, L. Urbain, P. Caron, S. Boudet, J. Gariépy, and J. Megnien. Hippocrate: A safe robot arm for medical applications with force feedback. *Medical Image Analysis*, 3(3):285–300, 1999. doi:10.1016/s1361-8415(99)80025-5.

[71] Alan Priester, Shyam Natarajan, and Martin Culjat. Robotic ultrasound systems in medicine. *IEEE Transactions on Ultrasonics, Ferroelectrics and Frequency Control*, 60(3):507–523, mar 2013. doi:10.1109/tuffc.2013.2593.

[72] Luigia Romano and Antonio Pinto Secaucus, editors. *Errors in Radiology*. Springer-Verlag Italia, 2012. doi:10.1148/radiol.14144004.

[73] S. Salcudean, G. Bell, S. Bachmann, W. Zhu, P. Abolmaesumi, and P. Lawrence. Robot-assisted diagnostic ultrasound–design and feasibility experiments. In *Medical Image Computing and Computer-Assisted Intervention–MICCAI'99*, pages 1062–1071. Springer, 1999. doi:10.1007/10704282_115.

[74] Conrad Sanderson. Armadillo: An Open Source C++ Linear Algebra Library for Fast Prototyping and Computationally Intensive Experiments. 2010.

[75] Bruno Siciliano, Lorenzo Sciavicco, Luigi Villani, and Giuseppe Oriolo. *Robotics: modelling, planning and control*. Springer London, 2009. doi:10.1007/978-1-84628-642-1.

[76] B.D. Sites, R. Brull, V.W.S. Chan, B.C. Spence, J. Gallagher, M.L. Beach, V.R. Sites, S. Abbas, and G.S. Hartman. Artifacts and pitfall errors associated with ultrasound-guided regional anesthesia. part ii: a pictorial approach to understanding and avoidance. *Regional anesthesia and pain medicine*, 32(5):419, 2007.

[77] B.D. Sites, R. Brull, V.W.S. Chan, B.C. Spence, J. Gallagher, M.L. Beach, V.R. Sites, and G.S. Hartman. Artifacts and pitfall errors associated with ultrasound-guided regional anesthesia. part i: understanding the basic principles of ultrasound physics and machine operations. *Regional anesthesia and pain medicine*, 32(5):412, 2007.

[78] Marian Uhercik, Jan Kybic, Hervé Liebgott, and Christian Cachard. Model fitting using ransac for surgical tool localization in 3-d ultrasound images. *Biomedical Engineering, IEEE Transactions on*, 57(8):1907–1916, 2010.

[79] P. Vieyres, G. Poisson, F. Courreges, O. Merigeaux, and P. Arbeille. The TERESA project: from space research to ground tele-echography. *Industrial Robot*, 30(1), 2003. doi:10.1108/01439910310457742.

[80] A. Vilchis, J. Troccaz, P. Cinquin, K. Masuda, and F. Pellissier. A new robot architecture for tele-echography. *Robotics and Automation, IEEE Transactions on*, 19(5):922 – 926, 2003. doi:10.1109/tra.2003.817509.

[81] A. Vilchis-Gonzales, J.C. Avila-Vilchis, A. Garcia-Torres, and J. Bernal. A robot for ultrasound examinations. In *IV Latin American Congress on Biomedical Engineering 2007, Bioengineering Solutions for Latin America Health*, pages 693–696, 2007. doi:10.1007/978-3-540-74471-9_161.

[82] A. Vilchis Gonzales, P. Cinquin, J. Troccaz, A. Guerraz, B. Hennion, F. Pellissier, P. Thorel, F. Courreges, A. Gourdon, G. Poisson, et al. TER: a system for Robotic Tele-Echography. In *Medical Image Computing and Computer-Assisted Intervention–MICCAI 2001*, pages 326–334, 2001.

[83] A. Vilchis-Gonzalez, JC Avila-Vilchis, and A. Garcia-Torres. Termi robot. In *Proceedings of the Electronics, Robotics and Automotive Mechanics Conference*, pages 464–469. IEEE Computer Society, 2007. doi:10.1109/cerma.2007.4367730.

[84] Marie-Aude Vitrani, Hubert Mitterhofer, Guillaume Morel, and Nicolas Bonnet. Robust ultrasound-based visual servoing for beating heart intracardiac surgery. In *Proceedings 2007 IEEE International Conference on Robotics and Automation*, pages 3021–3027. Institute of Electrical & Electronics Engineers (IEEE), apr 2007. doi:10.1109/robot.2007.363931.

[85] Gustaaf J. Vrooijink, Momen Abayazid, and Sarthak Misra. Real-time three-dimensional flexible needle tracking using two-dimensional ultrasound. In *2013 IEEE International Conference on Robotics and Automation*, pages 1680–1685. Institute of Electrical & Electronics Engineers (IEEE), may 2013. doi:10.1109/icra.2013.6630797.

[86] Ronald E. Walpole, Raymond H. Myers, Sharon L. Myers, and Keying Ye. *Probability & statistics for engineers & scientists*. Person Education, Inc., 8 edition, 2007.

[87] Z. Wei, L. Gardi, D.B. Downey, and A. Fenster. Oblique needle segmentation and tracking for 3d trus guided prostate brachytherapy. *Medical physics*, 32:2928, 2005.

[88] Zhouping Wei, Gang Wan, Lori Gardi, Gregory Mills, Donal Downey, and Aaron Fenster. Robot-assisted 3d-TRUS guided prostate brachytherapy: System integration and validation. *Med. Phys.*, 31(3):539–548, 2004. doi:10.1118/1.1645680.

[89] C.J. Zandsteeg, D.J.H. Bruijnen, and M.J.G. van de Molengraft. Haptic tele-operation system control design for the ultrasound task: A loop-shaping approach. *Mechatronics*, 20(7):767 – 777, 2010. Special Issue on Design and Control Methodologies in Telerobotics. doi:10.1016/j.mechatronics.2010.02.007.

[90] Yue Zhao, Adeline Bernard, Christian Cachard, and Hervé Liebgott. Biopsy needle localization and tracking using ROI-RK method. *Abstract and Applied Analysis*, 2014:1–7, 2014. doi:10.1155/2014/973147.